ABSTRACT

Title of Thesis: IMAGE-BASED SPECTROELECTROCHEMICAL FRAMEWORK TO PROBE REDOX-ACTIVE HYDROGELS

Mya Faith Hamstra
Master of Science in Bioengineering, 2026

Thesis Directed By: Dr. William E. Bentley

Robert E. Fischell Distinguished Chair in Engineering, Director of Robert E. Fischell Institute for Biomedical Devices, Director of Maryland Technology Enterprise Institute Professor, Institute for Bioscience and Biotechnology Professor, Fischell Department of Bioengineering

Spectroelectrochemistry integrates electrochemistry with optical spectroscopy and frequently employs chemometric analyses to understand relationships within complex chemical systems. Data generated from these techniques is high-dimensional and dense, requiring specialized expertise and advanced instrumentation to interpret. While these approaches provide powerful analytical capabilities, their cost and complexity can limit accessibility.

This thesis presents a simple, image-based analytical framework that extracts red, green, and blue (RGB) signals from time-resolved imaging to quantify chromogenic electrochemical

changes. To evaluate this approach, two catechol-functionalized polymer systems with distinct conjugation chemistries, catechol-modified chitosan (cat-chit) and catechol-functionalized polyethylene glycol (cat-PEG), were investigated. These systems were evaluated to compare fabrication and redox responsiveness. Measurements obtained through RGB image decomposition monitored optical and electrochemical changes while preserving complex spatial geometries at sub-second temporal resolution. The results demonstrate that this approach effectively captures analogous data to traditional spectrometry, providing a reliable and accessible alternative for probing complex electrochemical processes.

IMAGE-BASED SPECTROELECTROCHEMICAL FRAMEWORK TO PROBE REDOX-ACTIVE HYDROGELS

by

Mya Faith Hamstra

Thesis submitted to the Faculty of the Graduate School of the
University of Maryland, College Park, in partial fulfillment
of the requirements for the degree of
Master of Science,
Bioengineering,
2026

Advisory Committee:
Dr. William E. Bentley, Chair
Dr. Gregory F. Payne, Co-Chair
Dr. Yang Tao

Acknowledgements

Firstly, I would like to express my gratitude and appreciation to my principal investigator Dr. Gregory Payne who has been amazing to work with. From entering his lab via the Fischell Institute Internship Program, I knew immediately how lucky I was to be part of his group. I appreciated his trust in me to lead my own projects even as an undergraduate, and his overwhelming support and encouragement throughout the course of my Master's degree. His reassuring communication and utmost respect truly made me feel welcome every day.

Next, I would like to thank my committee members; Thank you to Dr. William Bentley for co-advising me throughout this journey and always offering welcoming support along the way. Thank you to Dr. Yang Tao for sparking my interest in device development through the senior capstone program. I truly appreciate your time and dedication to my work.

To Dr. Eunkyoung Kim: I can't thank you enough for your support and help throughout the past three years. Having someone to talk through ideas with and always giving me a hand when needed is something I will forever appreciate. Your excitement and approach to science have always inspired me and will continue to influence me throughout my career.

To Dr. Chen-Yu Chen: Thank you for always being so helpful and kind with all my crazy device ideas. I always appreciate your attention to detail and dedication to helping advance my work with your experienced 3D printing and device background.

To all of Dr. Bentley Lab and Fischell Institute: Thank you for always keeping the days interesting and providing such a welcoming community to work at every day. Being at the forefront of innovation where every conversation feels like a continual idea incubator is something I will always cherish.

Lastly, to my friends and family, thank you for your unwavering support and care throughout this process. Every failed experiment or idea breakthrough was always comforted or celebrated by you all, and I will forever be grateful for the continued encouragement.

Table of Contents

List of Figures

List of Abbreviations

Cat-chit: Catechol-modified chitosan

Cat-PEG: Catechol-functionalized PEG

CV: Cyclic Voltammetry

ROI: Regions of Interest

RGB: Red, Green, Blue

Chapter 1: Introduction

Aim and Scope of Thesis

To explore catechol conjugation and redox behavior in controlled environments, two polymer systems with distinct grafting chemistries were investigated. Catechol modified chitosan (cat-chit) and catechol-functionalized polyethylene glycol (cat-PEG) were used to represent both amine and thiol rich reaction systems relevant to catecholic structures in biology[1,2]. By comparing these two platforms, fabrication/grafting and redox-responsive behaviors can be monitored in relation to their underlying conjugation chemistries.

To monitor and analyze these systems, a new image-based red, green, and blue (RGB) analysis framework was developed to quantify fluorochromogenic and chromogenic electrochemical changes through digital imaging. This method leverages time-resolved image acquisition and RGB channel decomposition to simplify complex optical responses to accessible molecular signals while preserving both temporal and spatial information. By applying this framework to catechol-functionalized polymer networks, **this thesis aims to evaluate the fabrication and redox behavior of two distinct systems while demonstrating the utility of RGB-based image analysis as a tool for probing catecholic electrochemical systems.**

Catecholic Materials in Biology

Catechols represent a versatile class of redox-active organic molecules, enabling a wide range of chemical transformations[3]. These molecules readily undergo reversible oxidation to form quinones (**Fig. 1.1**), which can subsequently participate in nucleophilic addition[4], crosslinking[5], and similar interactions. As a result, catechol chemistry is central to numerous biological

material systems, especially in processes like adhesion[6], redox cycling[7], and polymer formation[8]. The reactivity of catechol and quinone intermediates is highly dependent on the surrounding chemical environment[9], including the presence of nucleophiles like amines and thiols, which can produce distinct conjugation pathways and material properties.

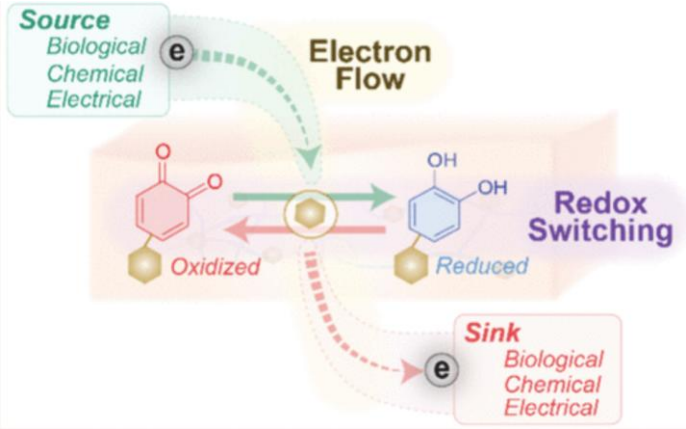

Figure 1.1: Catechol redox switching putative reaction[10]

Melanins are a diverse class of pigments produced by melanocytes and are primarily found in the skin, hair, and eyes[11]. Beyond their role in pigmentation, they possess various functional attributes including photoprotection[12], redox activity[13], and metal ion chelation[14]. Despite their ubiquitous expression in biology, melanins remain comparatively understudied due to the limited mechanistic understanding of their polymerization process and the inherent structural heterogeneity of the resulting polymers[15].

Among the different types of melanin, eumelanin and pheomelanin represent the two most important classes in determining pigmentation[16]. Eumelanin is responsible for the brown/black pigment while pheomelanin dominates the red/yellow undertones[17]. As a result, varying ratios of these two types of melanin strongly influence skin, hair, and eye color[18]. Although both classes

originate from catechol-based precursors derived from L-DOPA, their polymerization pathways diverge through two distinct conjugation chemistries.

These structural differences arise from variations in underlying biosynthetic pathways that govern conjugation and subsequent polymerization (**Fig. 1.2**)[19]. Pheomelanin (**Fig. 1.2a**) formation is strongly governed by sulfhydryl-containing molecules such as cysteine, which react with DOPA-quinone to produce intermediates that ultimately polymerize into pheomelanin[20]. In contrast, eumelanin (**Fig. 1.2b**) formation proceeds through similar oxidative intermediates but occurs in the absence of cysteine. Rather, DOPA-quinone undergoes a reaction to form dopachrome intermediates, ultimately generating eumelanin structures rich in amine groups[21].

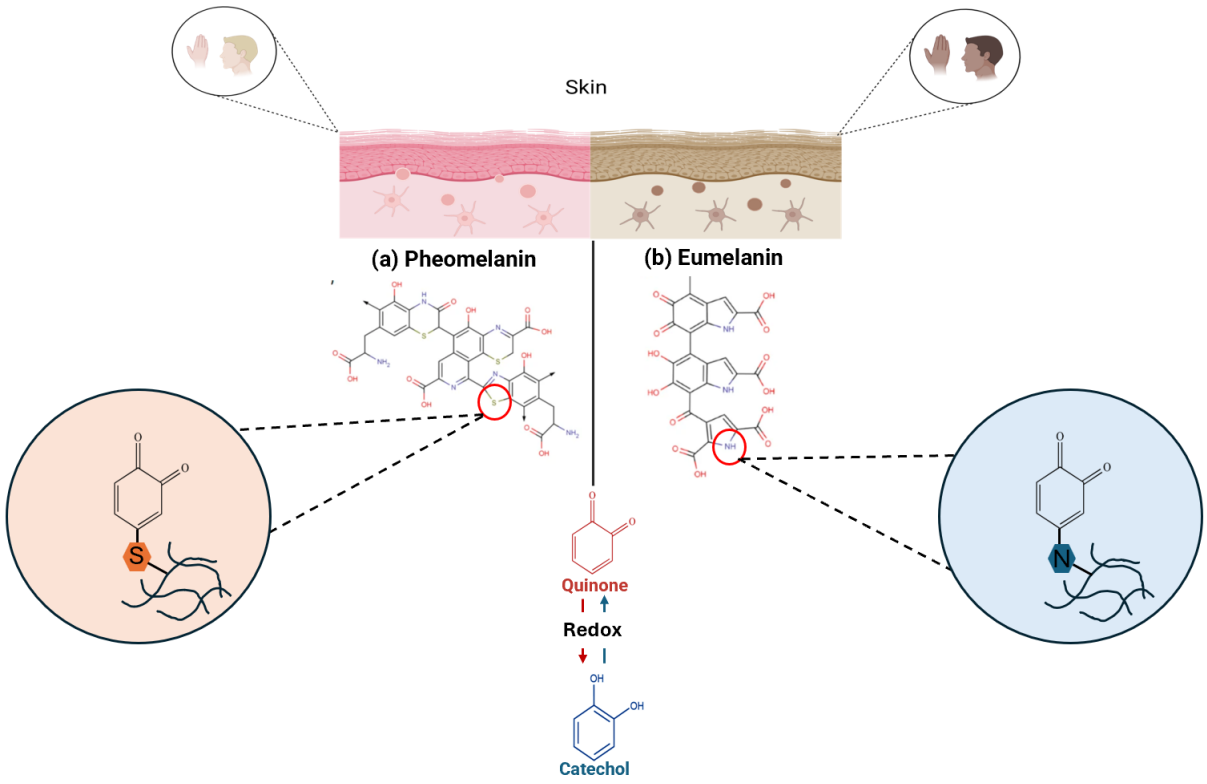

Figure 1.2: Catechol in Biology. Catechol is observed in both pheomelanin (left) and eumelanin (right).

Catecholic Polymers in Biotechnology

Due to the heterogenous, insoluble, and structurally complex nature of melanins, directly studying the chemical processes that govern their formation and redox behavior remains a challenge. As a result, catechol chemistry derived from melanin precursors has increasingly inspired the development of functional biomaterials that leverage the unique redox and adhesive properties of catechol groups[22,23]. These catechol-functionalized polymers have emerged as versatile platforms to create tunable materials with applications in surface coatings[24], bioadhesion[25], and electrochemical interfaces[26]. Polymers such as cat-chit and cat-PEG provide chemically well-defined systems in which catechol grafting strategies and redox behavior can be systematically investigated[27,28]. Furthermore, the chromogenic and fluorochromogenic nature of catechol oxidation and reduction makes these systems especially suitable for both electrical and optical analyses[29].

Spectroelectrochemical Tools

Despite these advances, accessible analytical approaches for monitoring catechol conjugation reactions remain limited. Notably, spectroelectrochemistry has offered a fresh perspective in the field by enabling operando measurement of both electrical and optical signals during reaction progression[30]. This approach allows chemical transformations to be monitored in real time via two distinct modalities, providing insight into how redox influences molecular changes that can be observed via optical responses such as absorbance or fluorescence changes[31]. However, this tool typically generates large multidimensional datasets consisting of full spectral information collected at sub-second time scales. Processing and interpreting such datasets often require deconvolution of data with specialized instrumentation, which is often time intensive and resource demanding[32].

To address the high data volume and time-consuming analyses in alternative analytical approaches, this thesis explores image-based RGB analysis as a rapid and accessible method for monitoring both the fabrication and redox properties of catecholic materials. By decomposing images into their red, green, and blue (RGB) components, subtle changes in pigment formation can be potentially monitored without the use of full spectral equipment[33]. Catechol-functionalized polymer systems, including cat-chit and cat-PEG, were used as biomimetic reaction platforms to represent amine and thiol rich environments; two important conjugations in catechol biomaterials[34]. By correlating changes in RGB signal with reaction progression, this study aims to evaluate whether digital image analysis can serve as a practical alternative for probing catechol conjugation and redox processes.

Putative Grafting Reactions

When creating these redox-active hydrogels (**Fig. 1.3**) to monitor fabrication chemistries, both cat-chit and cat-PEG will undergo a series of procedures. Chitosan uses a two-step deposition process whereas PEG only utilizes one step.

Cat-Chit Modification Reaction

Chitosan, a pH-responsive polysaccharide, can be easily electroassembled at the electrode surface via a reversible cathodic electrodeposition step. However, due to the voltage range specifications of electrodes used in the latter experiments, cathodic electroassembly is not viable. As a result, chitosan casting followed with catechol modification (seen in **Fig. 1.3a**) will be the standard protocol in these experiments. This procedure starts with 1% chitosan added to the working electrode surface, followed by a drying period in which all water has been evaporated from the system. Once a thin film has dried onto the working electrode, a solution of 0.1M

sodium hydroxide (NaOH) is placed over the chitosan film for 15 minutes. Addition of NaOH neutralizes the acidic chitosan, deprotonating and therefore inducing gelation to create a compact film on the electrode. After gelation, the film is rinsed with phosphate buffer (PB) and placed in a solution of 50mM catechol, where an anodic potential is applied to actively graft catechol to the amine groups located on the chitosan. Following this step, a chitosan-modified catechol film is created.

Cat-PEG Functionalization Reaction

PEG, a water-soluble polymer known for its biocompatible nature, is often used in electrochemical materials for its versatility and wide potential domains. Largely due to the presence of thiol groups and their reactivity, PEG can be co-deposited with catechol, both using anodic depositions to be functionalized onto the electrode. The procedure starts by adding a solution of 50mM catechol and 50 mg/mL 4-arm thiol polyethylene glycol to the surface of a working electrode. Inducing an anodic potential triggers oxidation, generating quinones at the electrode surface which then can react with reactive -SH groups on PEG, controllably generating networked cat-PEG onto the surface of the electrode. While the exact mechanism of catechol functionalization to PEG is unknown, it appears that three things could be occurring: oxidative formation of S-S crosslinks, quinone-based grafting to nucleophilic SH groups, or quinone-based crosslinking. Due to the uncertainty of an underlying mechanism, a putative reaction is shown in **Fig. 1.3b**.

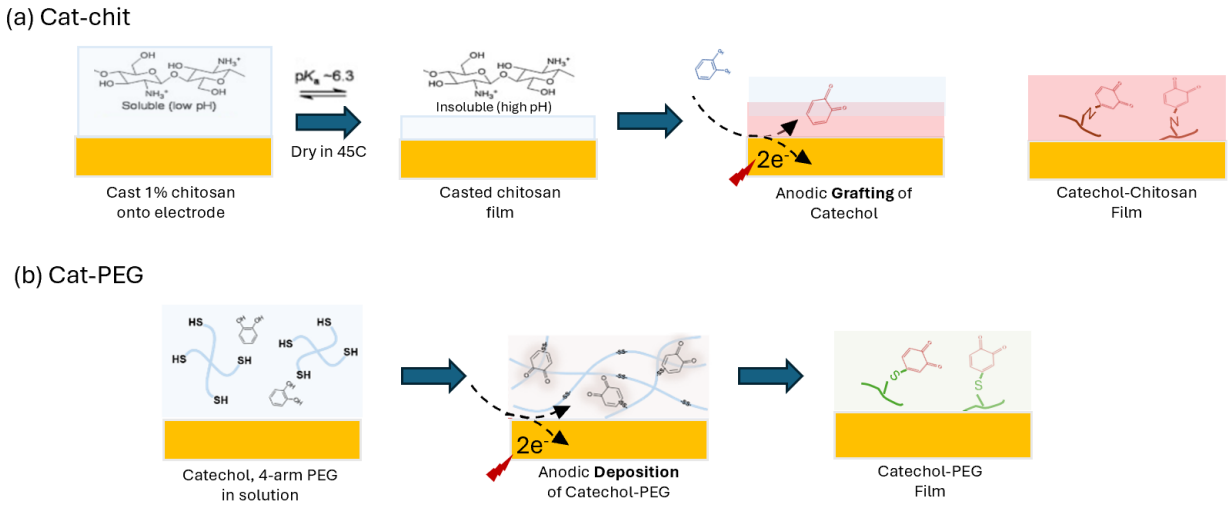

Figure 1.3: Putative grafting reactions of (a) cat-chit and (b) cat-PEG[10,35]. Materials and extensive procedure outlined in experimental methods chapter.

Features of Image Analysis Framework

Based upon the challenges associated with dense datasets and intense data processing, image-based RGB analysis offers a simplified and accessible approach for monitoring chromogenic electrochemical systems[36]. By capturing digital images during reaction progression or redox switching and composing them into RGB data, complex spectral information can be reduced into a small set of quantifiable parameters. This approach offers three key features: **spectral decomposition (Fig. 1.4 left), temporal monitoring (Fig. 1.4 middle), and spatial resolution (Fig. 1.4 right).**

Spectral Simplification Through RGB Decomposition

In standard full-spectrum analyzers, a full absorbance spectrum is generated for each time point. Due to the rapid nature of electrochemical reactions, time intervals typically lie within the millisecond range[37]. These intervals, coupled with spectral data can yield huge data sets of both optical and electrical information. However, moieties relevant to catechol-functionalized fabrication or redox cycling may only be active at certain wavelength ranges[38]. This approach

enables rapid interpretation of optical changes without the need for full spectral acquisition and intensive data processing. RGB decomposition simplifies the complex spectral information into discrete color channels or filters that cover wide wavelength ranges. When moieties can be characterized through these filters, the need for full spectral acquisition and extensive post processing diminishes.

Temporal Monitoring of Electrochemical Reactions

Electrochemical processes are widely used both for the fabrication of functional materials and for characterizing the redox behavior of previously prepared systems, making it essential to monitor chemical changes as they occur[39]. Spectroelectrochemistry provides a powerful framework for this purpose by coupling electrochemical control with optical measurements, enabling operando observation of both electrical and molecular responses[30]. While typical chemical reactions proceed rapidly, electrochemical systems offer the advantage of precisely controlled environments in which a defined number of electrons can be introduced or removed from a system. Monitoring these redox-driven changes as a function of time is therefore critical for understanding internal reactions of electrochemically fabricated materials.

The RGB-based image analysis framework developed in this work enables high-resolution temporal monitoring of these processes through time-resolved image acquisition. By capturing images at customizable frame rates via external imaging software, this approach allows for the tracking of optical deviations throughout an electrochemical experiment. As a result, the method can achieve better temporal resolution compared to commercial spectrometers, which are often limited by their photon accumulation rates and internal hardware motion[40].

Spatially Resolved Analysis of Electrode Geometries

In addition to temporal monitoring, spatial resolution is also a critical advantage of image-based analysis. Conventional spectroscopy and electrochemical instruments typically provide average signals over an entire electrode surface, making it difficult to detect localized variations in molecular or optical response[41]. However, advanced electrode geometries and surface redox states can induce highly specific localized chemical activity, in which certain regions exhibit enhanced optical changes while others remain inactive[42]. By preserving spatial information across the entirety of the electrode, this RGB-based image analysis framework enabled direct visualization and quantification of these geometrically distinct responses, allowing conversation between electrode geometry and redox behavior to be explored in real time. This approach provides a level of resolution unattainable within traditional bulk spectral measurements, particularly in patterned electrode systems.

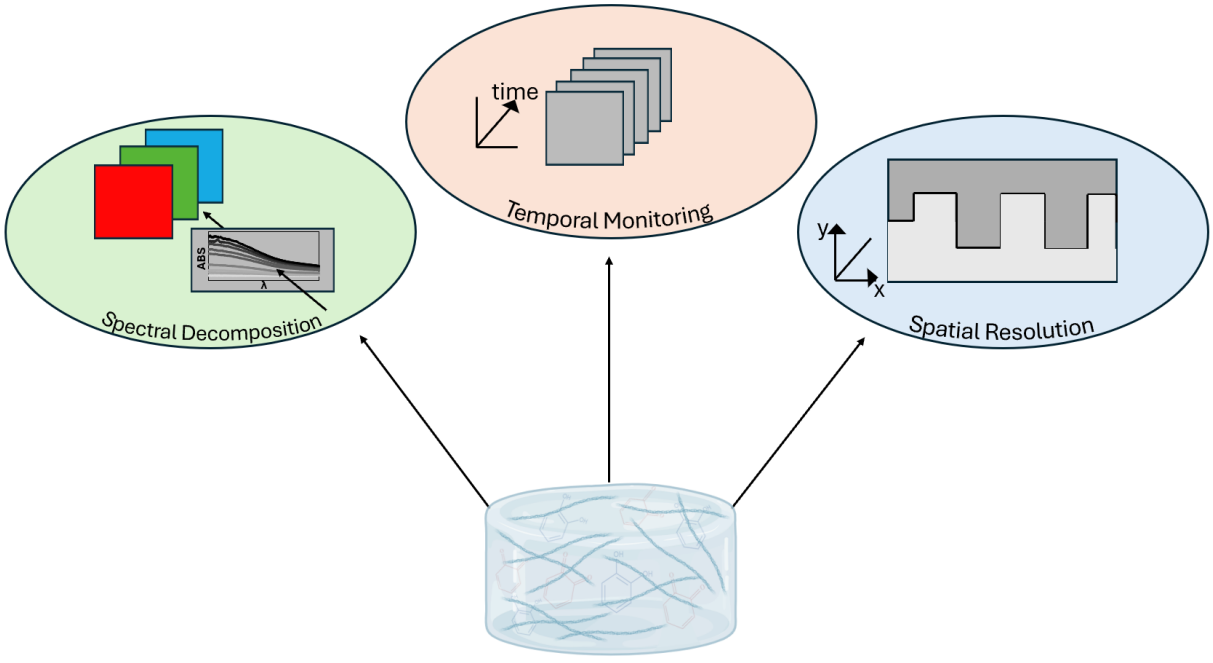

Figure 1.4: Features of RGB-Based Image Analysis Framework. Spectral decomposition to measure materials in three distinct color channels, temporal monitoring to dynamically measure reaction progression, spatial resolution allowing for localized measurements across an electrode surface.

Chapter 2: Experimental Methods

Camera-Based Experimental Setup

4-Well 3D Printed Spectroelectrochemical Platform

To enable operando microscopy through image-based analysis, a fluorescence microscope is used to visualize optical changes in the system during electrochemical operations. These experiments employ a spectroelectrochemical device previously developed in our laboratory[35] (**Fig. 2.1**), which allows simultaneous electrical control while capturing top-down, time-resolved images of the electrode surface.

The device consists of a 3D printed housing containing four independent wells, enabling higher-throughput experimentation compared to the conventional single-sample cuvette configuration commonly used in spectrometers. This housing is affixed to laser-engraved indium tin oxide (ITO) coated glass using photothermal resin. This resin acts as a sealant between the housing and the conductive substrate, isolating each well so that it functions as an individual working electrode.

Following assembly, 65uL of agarose is pipetted into the central well of the device and overlaid with potassium chloride (KCl) solution. This configuration serves as a salt bridge that connects the central electrolyte reservoir to each of the four samples wells through small vents located at the base of each channel. A platinum counter electrode and an Ag/AgCl reference electrode are then inserted into the KCl reservoir, allowing a single counter/reference pair to service all four working electrodes simultaneously.

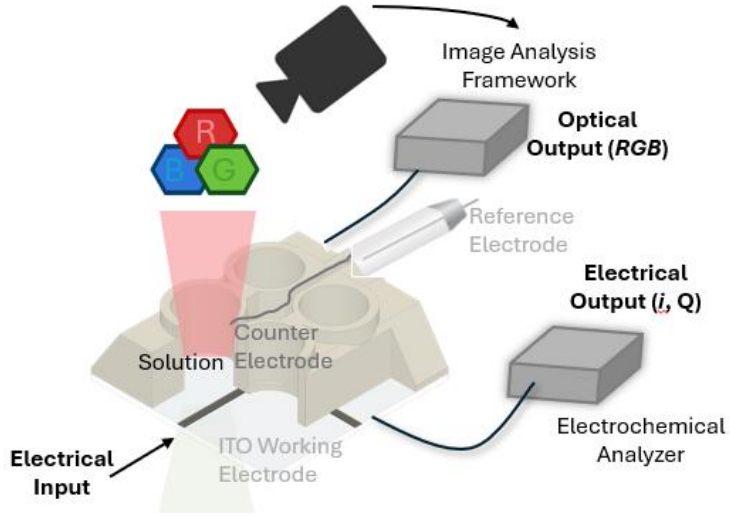

Figure 2.1: Camera-Based Experimental Setup. Four independently addressable working electrodes (ITO), singular counter and reference electrodes shared between all wells through an agarose-salt bridge.

Dynamic Camera Imaging

Following fabrication of the 4-well ITO spectroelectrochemical device, the platform is secured within a custom docking station equipped with four independent working electrode connections and a shared counter and reference electrode. The docking station is then positioned beneath a fluorescence microscope fitted with a digital camera to enable continuous video-based image acquisition during electrochemical experiments.

Electrochemical measurements are performed using an electrochemical analyzer (CHI Instruments). Simultaneously, screen-recording software (Camtasia, TechSmith) is used to capture the live camera output from the microscope, generating a time-resolved video of the electrode surface throughput the experiment. Upon completion of the experiment, both the electrochemical data file and the recorded video are exported for further analysis. These datasets can be synchronized and segmented at user-defined time intervals, enabling customized temporal and spatial resolution for image-based analysis.

Absorbance Monitoring

For absorbance-based measurements, broadband white light is directed though the bottom of the spectroelectrochemical platform, allowing optical changes at the electrode surface to be monitored from a top-down perspective. Prior to initiating the electrochemical experiments, a background correction is performed by capturing an image of the illuminated device without active redox processes. This white-light background is then used for subtraction during data analysis to ensure that measured absorbance changes arise solely from the formation or transformation of molecular species within the hydrogel.

Fluorescence Monitoring

For fluorescence measurements, a light-absorbing material is placed beneath the spectroelectrochemical platform to minimize reflected excitation light. The system is then illuminated using a fluorescence excitation filter at an excitation wavelength of 440 nm, and emission intensity is monitored though a corresponding emission filter at 520 nm during electrochemical measurements. Changes in fluorescence intensity are recorded continuously by the camera and later analyzed using the RGB image-based workflow.

Image Analysis Workflow

Experimental Setup

The 4-well spectroelectrochemical device was fabricated following the procedures described above and subsequently loaded into its custom docking station (**Fig. 2.2a**). This docking station was then placed on the stage of a fluorescence microscope and connected to the working, counter, and reference electrode leads of the CHI electrochemical analyzer. In this configuration,

a clear top-down view of the four sample channels was obtained for optical monitoring. Depending on measurement mode, either bottom-up broadband white light or top-down fluorescent excitation filters were applied to the system to enable absorbance or fluorescence measurements, respectively.

ImageJ Partitioning

Following completion of the electrochemical experiment, the recorded video was exported in .avi format for image processing. A custom ImageJ macro developed for this project was then used to analyze the video by separating each frame into its three color channels: red, green, and blue. Based on the user-selected channel of interest, the macro retained the desired color channel while discarding the remaining two channels.

Once the video frames were reduced to a single color channel, predefined regions of interest (ROIs) were applied to each sample channel. Five square ROIs (see **Fig. 2.2b**) arranged in a cross-shaped pattern were selected for each electrode. The macro then calculated the average intensity of these five regions to generate a single intensity measurement for each channel at every frame. As the macro iterated through the entire video, these measurements were collected sequentially, resulting in a time-dependent optical dataset for each electrode channel.

The selection of five ROIs was intended to account for potential heterogeneity within the hydrogel films. When thin hydrogels are fabricated on circular electrode surfaces, partial delamination or peeling can occur near the electrode edges where the hydrogel interfaces with the surrounding housing. To minimize the influence of these edge effects, ROIs were positioned toward the interior region of the electrode surface, ensuring that measurements were collected from the most uniform portion of each hydrogel.

Data Acquisition

During image processing, the averaged intensity values obtained for each channel were converted into absorbance measurements using a modified form of the Beer-Lambert relationship (**Fig. 2.2c**). In this approach, the intensity recorded in the first frame of the experiment was treated as the initial light intensity (I_0). For each subsequent frame, the measured intensity (I) was normalized relative to I_0, and the absorbance was calculated using the logarithmic relationship[43]:

$ABS = \log (I_0 / I)$

This transformation allowed the optical changes captured by the camera to be expressed in absorbance units, enabling quantitative comparison with traditional spectroscopic measurements.

Temporal Monitoring

The ImageJ macro was designed to process every frame of the recorded video, enabling continuous time-resolved analysis throughout the electrochemical experiment. Temporal resolution could be adjusted by modifying the video frame rate during image acquisition using external recording software. Ideally, the frame rate was selected to match the temporal resolution of the electrochemical data output, allowing optical and electrical signals to be directly correlated at corresponding time points. This synchronized analysis enables simultaneous interpretation of both the redox behavior and molecular changes occurring within a system.

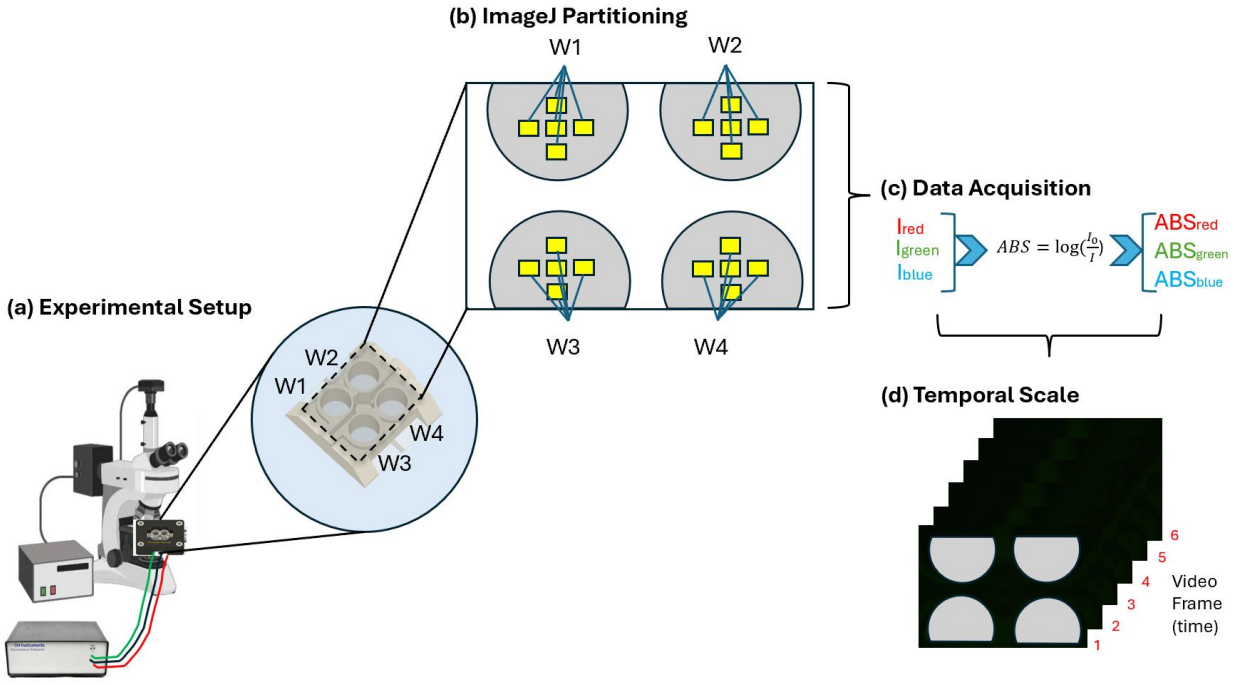

Figure 2.2: RGB-based Image Analysis Framework. (a) experimental setup of 3D printed device fitting into instrumentation, (b) geometrical partitioning of 5 separate data values averages into a singular global intensity per well, (c) conversion of global intensities (in each color channel) into absorbance measurements, (d) iteration through each frame in a video recording.

Fabricating catechol functionalized hydrogels

Cat-chit

Cat-chit hydrogels were fabricated using a two-step electrografting process. First, a thin film of chitosan was cast onto the surface of the working electrode and subsequently neutralized to form a stable hydrogel layer. Following film formation, catechol groups were grafted onto the chitosan matrix through an anodic electrografting step.

Within the camera-based image analysis framework, a constant potential of +1.0V was applied for 5 minutes (300 s) to induce catechol grafting onto the pre-formed chitosan film.

Cat-PEG

Cat-PEG hydrogels were fabricated using a one-step electrodeposition process. In this approach, a precursor solution containing 50mM catechol and 50 mg mL^{-1} 4-arm thiol PEG was

simultaneously deposited onto the electrode surface through an anodic potential step. The electrochemical oxidation of catechol promotes thiol-quinone coupling reactions, resulting in formation of a catechol-functionalized PEG hydrogel at the electrode surface.

For experiments performed within the camera-based image analysis setup, a constant potential of +1.0V was applied for 5 minutes (300 s) to generate hydrogel films.

Redox probing catechol functionalized hydrogels

Cyclic Voltammogram

Following hydrogel fabrication, the deposition solution was removed from each electrode (leaving only the insoluble hydrogel) and incubated with phosphate buffer (PB) for 30 minutes. This incubation step allows unreacted catechol species remaining in the hydrogel matrix to diffuse out of the film and into the surrounding buffer, which was subsequently discarded. After the washing step, a 150 uL solution of 0.5 mM 1,1′-Ferrocenedimethanol (Fc) and 0.5 mM $Ru(NH_3)_6Cl_3$ ($Ru\ 3^+$) was added to each electrode. Cyclic voltammetry (CV) measurements were then performed at a scan rate of 5 mV s^{-1} for three cycles. Within the camera-based electrochemical imaging setup, a potential window of -0.6V to +1.0V was swept.

Chapter 3: Fabrication of Catecholic Hydrogels

To evaluate the performance and reliability of the proposed RGB-based image analysis framework during fabrication and redox-dependent absorbance monitoring, a spectroelectrochemical instrument was used as the reference device. This comparison enables the assessment of the trade-offs between reduced spectral resolution in RGB analysis and the gain in both temporal and spatial resolution offered by image-based methods. In this context, spectroscopic measurements serve as a benchmark for validating the ability of the RGB framework to capture key optical and redox features of the systems. Experiments conducted using the reference instrument were analogous to those completed in the camera-based setup, with minor alterations to procedures and materials outlined below.

Ground Truth Device

The instrument used in this study was a WaveNow Wireless electrochemical workstation (Pine Research Instruments), enabling simultaneous electrochemical control and optical measurement. This system allows for the operando monitoring of absorbance changes during electrochemical experiments by integrating electronic input with wavelength-resolve spectral detection[44].

The spectrometer operates using a conventional cuvette-based configuration (**Fig. 3.1**), in which a focused light beam is transmitted through a sample and the resulting absorbance is calculated using the Beer-Lambert relationship[44]. Experiments performed in this platform utilized a transparent gold working electrode in a three-electrode system consisting of a working, counter, and reference electrode. The integrated gold electrode served as both the working and counter electrodes, while an external Ag/AgCl electrode was used as the reference.

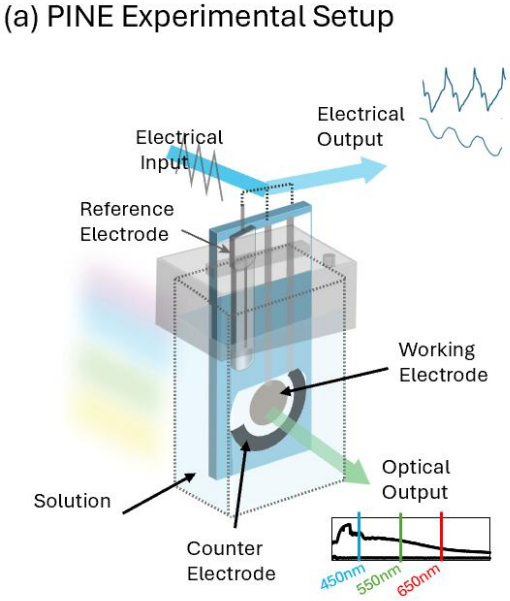

Figure 3.1: Pine Experimental Setup. Cuvette system with counter and working electrodes from a transparent gold electrode and an external reference electrode (Ag vs/ Ag/Cl).

Pine Instrument Methods

Fabrication: Hydrogel fabrication procedures were adapted from those described in the experimental methods section for use with the Pine instrument (**Fig. 3.2**). Due to differences in both electrode surface area and material between the camera-based platform (ITO) and the Pine Instrument (transparent gold), deposition parameters were adjusted to achieve comparable hydrogel formation across both systems. Specifically, deposition time and/or total charge delivered were modified to enable a more direct comparison of material properties.

For cat-chit, an anodic potential of +1.0V was applied for approximately 55s, corresponding to a total charge of ~28mC. For cat-PEG, potential was applied at +1.0V for approximately 90s, corresponding to a total charge of ~42mC.

Cyclic Voltammogram: CV measurements were performed over different potential windows depending on the experimental platform. In the camera-based imaging setup, a potential range of

-0.6V to +1.0V was applied. In contrast, the Pine instrument utilized a narrower potential window of -0.5V to +0.6V, consistent with the operational constraints of the transparent gold electrode configuration.

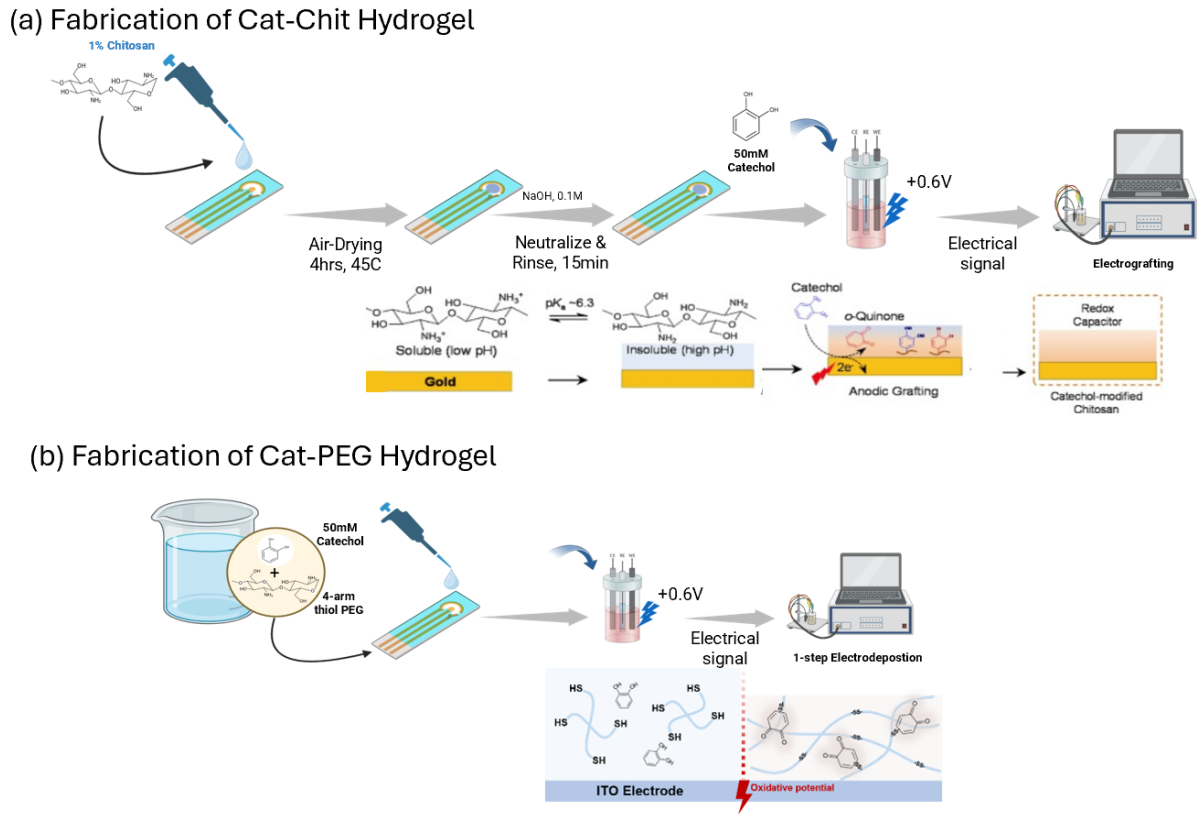

Figure 3.2: Fabrication Procedures on Transparent Gold Electrode. (a) Cat-chit and (b) cat-PEG fabrication.

Data Mapping Between Methods

To enable direct comparison between image-based RGB analysis and spectroscopic measurements, spectral data were mapped onto the RGB color space using literature-reported representative wavelengths for each color channel[45] **(Fig. 3.3)**. Specifically, discrete wavelengths corresponding to red, green, and blue optical regions were selected based on prior reports, and absorbance values at these wavelengths were extracted from the spectra dataset.

In this work, wavelengths of 450nm, 550nm, and 650nm were used to represent the blue, green, and red channels respectively[46] (**Fig. 3.3**). This approach establishes a consistent and physically meaningful correspondence between wavelength-resolved spectral measurements and the discrete color channels obtained from RGB image analysis.

By reducing spectral data to these representative wavelengths, direct comparison between the two methods is achieved, allowing for validation of the RGB-based image analysis framework while preserving optical trends observed in full spectral data.

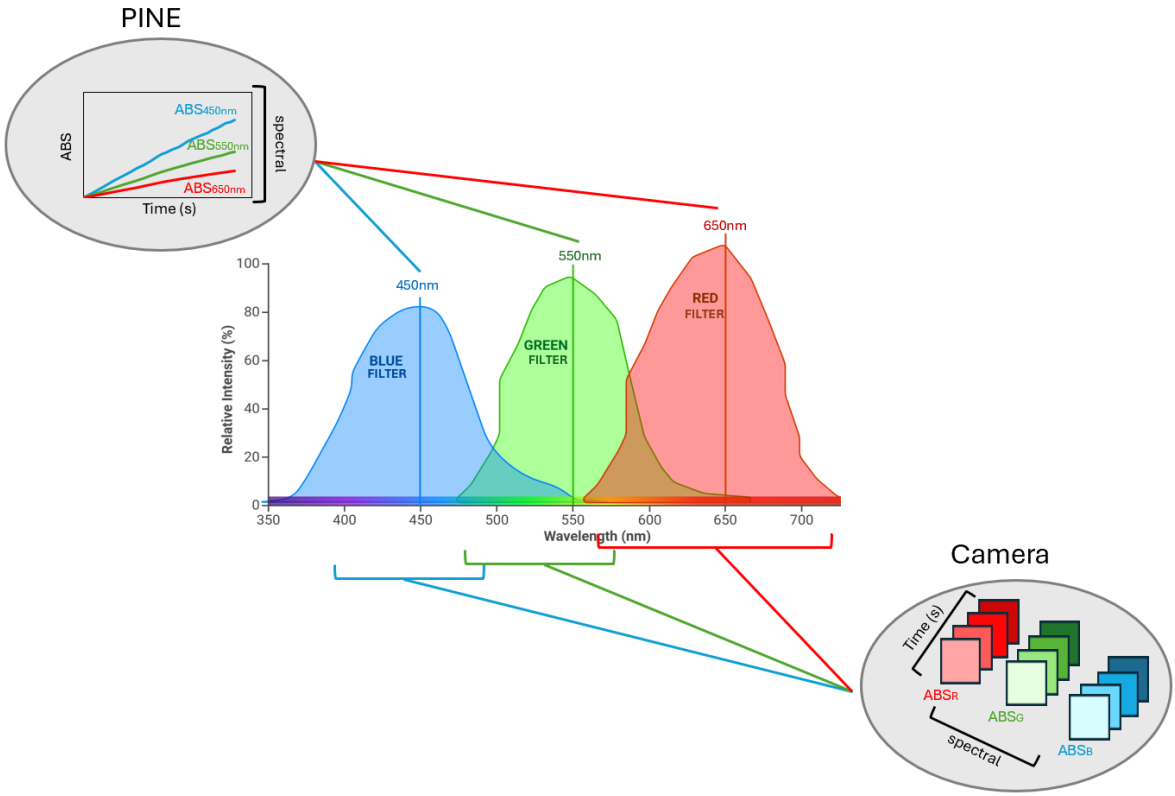

Figure 3.3: Data Output Between Devices

Temporal Monitoring of Fabrication

Emergence of Optical Information

During electrochemical fabrication, both electrical and optical measurements provide complementary insight into material formation. The total charge passed during deposition (Q_{fab}) reflects the extent of electrochemical oxidation used to induce fabrication, while optical measurements capture changes associated with molecular features and polymerization. By combining these two modalities, fabrication can be monitored in real time, enabling direct comparison between the camera-based image analysis framework and the spectroelectrochemical reference instrument.

Data Normalization and Visualization

As fabrication progresses, the electrode is withdrawing electrons from catechol to generate quinone which undergoes a reaction with either chitosan or PEG-thiols. The cumulative charge (Q_{fab}) is a measurement of that oxidation capacity and increases with time, with the final value corresponding to the total charge required to form the hydrogel (**Fig. 3.4**). Simultaneously, reaction products of the electrochemical reaction are responsible for the changing or emerging optical absorbance detected by either the Pine instrument or camera. While both time and charge evolve simultaneously, charge provides a more meaningful basis for comparison between samples, as it directly reflects the electrochemical input driving material formation.

To account for differences in total charge across experiments, the fabrication process was normalized using a dimensionless parameter representing the extent of modification (Q_{mod}), defined as:

$$Q_{mod} = \left(\frac{Q_i}{Q_{end}}\right) * 100$$

Where Q_i is the charge at a given time point and Q_{end} is the total charge at the end of fabrication. This normalization enables direct comparison of fabrication progress across different systems and experimental conditions.

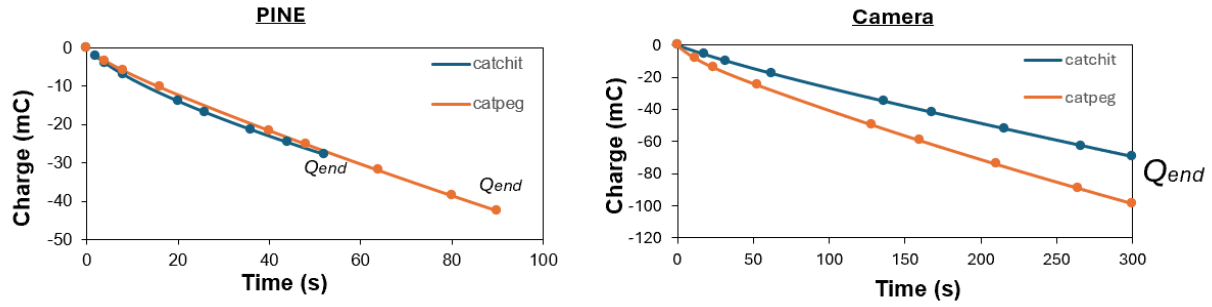

Figure 3.4: Charge-Time Plots of Fabrication. Q_{end} denotes total charge accumulated to generate the material.

Because operando measurements were performed using both optical and electrochemical techniques, the resulting dataset consists of three dimensions: absorbance (or optical response), wavelength (or RGB channel), and extent of modification (Q_{mod}). **Fig. 3.5** illustrates this relationship through three-dimensional representations of cat-chit and cat-PEG fabrication, where full spectral evolution is visualized at discrete Q_{mod} intervals. Corresponding RGB channel data and representative wavelengths are overlaid to highlight the connection between simplified color-based analysis and wavelength resolved spectral measurements.

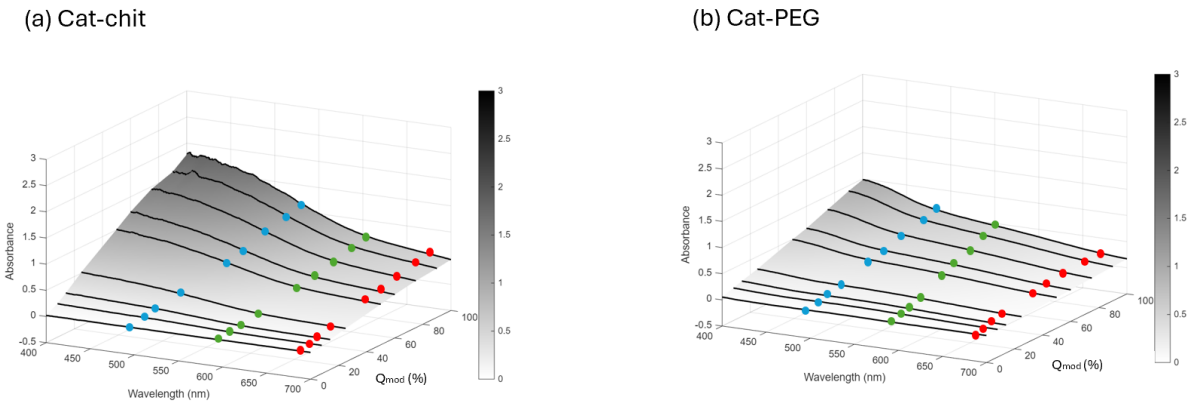

Figure 3.5: 3D Fabrication Plots

Cross-Modal Fabrication Correlation

Absorbance-Charge Information

To investigate the relationship between electrochemical input and optical response, absorbance was plotted as a function of accumulated charge. This approach enables direct comparison of how optical signals evolve relative to the extent of electrochemical fabrication.

Fig. 3.6a presents the absorbance-charge profiles obtained with the Pine instrument, where absorbance is tracked at three representative wavelengths corresponding to the RGB regions of the spectrum. **Fig. 3.6b** shows the absorbance-charge behavior obtained from the camera-based image analysis framework, where optical signals are derived from RGB color filters.

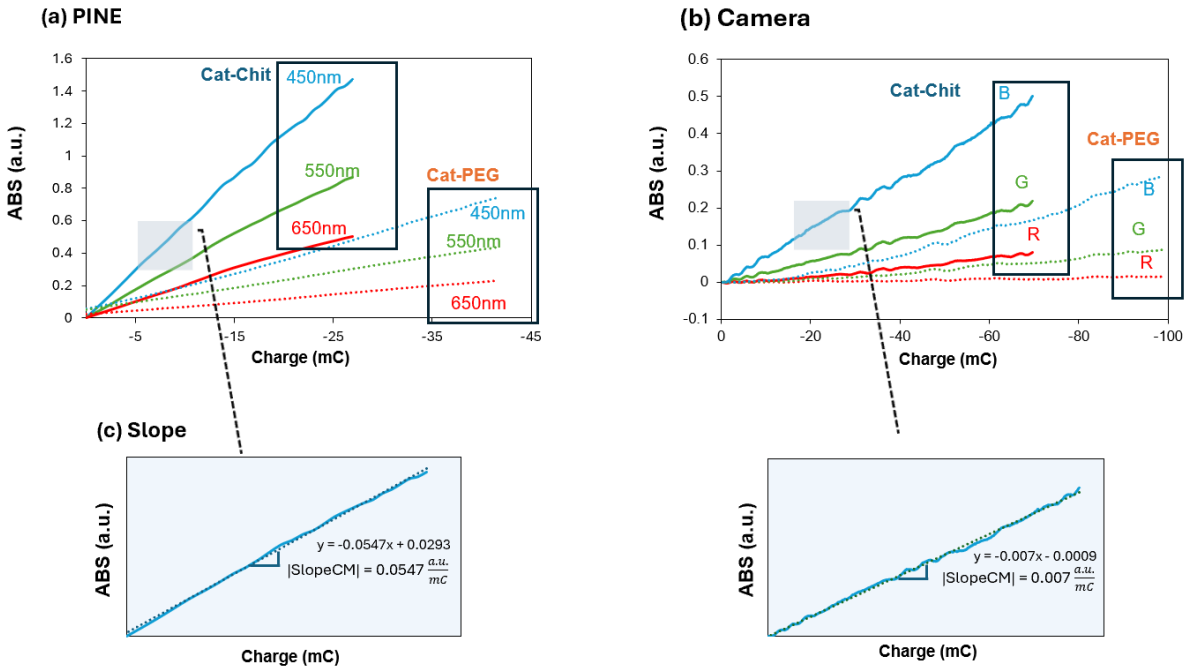

Figure 3.6: Fabrication Comparison. $Slope_{CM}$ was calculated for each individual wavelength/color by calculating the slope of the line.

The primary objective of this analysis was to quantify the relationship between optical responses measured on the Pine instrument and those obtained from the RGB-based image analysis

framework during fabrication. To deduce this comparison, data was reduced to a single parameter defined as the cross-modal slope ($Slope_{CM}$) (illustrated in **Fig. 3.6c**), which described the rate of change in absorbance as a function of accumulated charge for each wavelength or color channel.

$$Slope_{CM} = \frac{\Delta ABS}{\Delta Q}$$

This parameter captures the rate in which absorbance accumulates during fabrication, providing a direct measure of how rapidly absorbance increases with electrochemical input (**Fig. 3.6c**). By comparing $Slope_{CM}$ values across both wavelength-resolved spectral data and RGB channels, the consistency between both approaches can be evaluated.

Because the underlying mechanisms of catechol conjugation to thiol and amine functionalities remain incompletely understood, this approach may also provide insight into wavelength regions or color channels that are particularly sensitive to changes in molecular structure during fabrication. Broadly speaking, this analysis enables evaluation of whether simplified RGB-based measurements can capture the same charge-dependent optical trends seen in full spectral datasets.

Cross-Modal Correlation

Once $Slope_{CM}$ values were calculated for each representative wavelength in the Pine instrument and each RGB filter in the camera-based setup, a correlation analysis was performed to evaluate the degree of agreements between the two approaches (**Fig. 3.7**).

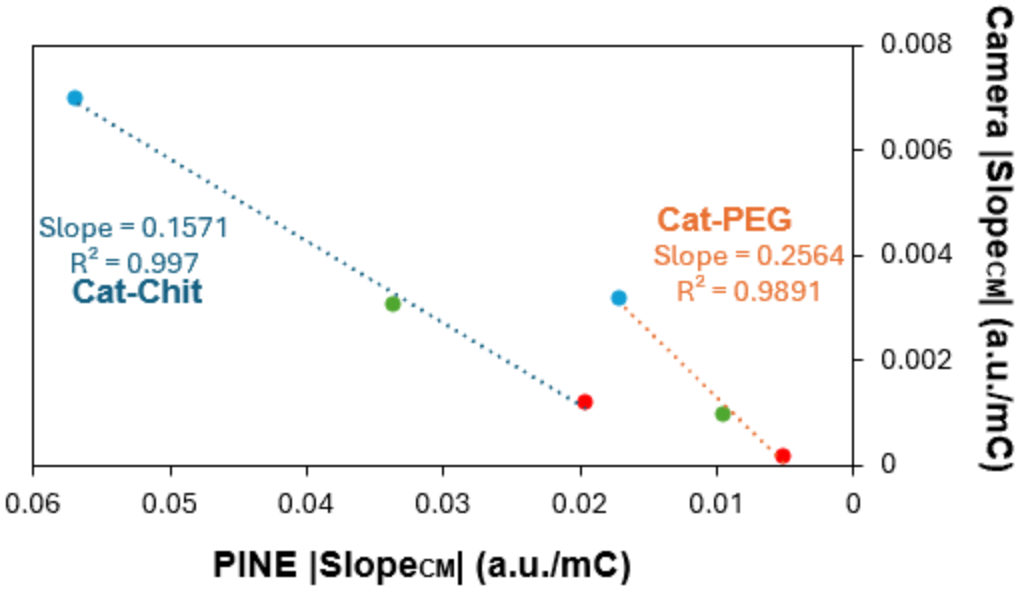

Figure 3.7: Cross-Modal Correlation using each respective color's $Slope_{CM}$ plotted against each other in either instrument.

The resulting correlation plots demonstrate a strong linear relationship between the Pine instrument measurements and the camera-based image analysis for both Cat-chit and Cat-PEG systems, with coefficients of determination (R^2) exceeding 0.98. These high R^2 values indicate that over 98% of the variance in the RGB-derived data is explained by the corresponding spectral measurements, highlighting a high degree of agreement between both methods.

A strong correlation suggests that the RGB-based image analysis framework reliably captures the charge dependent emergence of optical signals observed in wavelength-resolved spectral information. Consequently, the simplified RGB analysis approach can reproduce key trends in how different optical regions evolve during electrochemical fabrication of catechol-functionalized hydrogels.

Chapter 4: Temporal Analysis of Redox Switching

Motivation

Electrochemical redox cycling is widely used to interrogate the reversible nature of redox-active materials, providing insight into electron transfer kinetics, material stability, and function characterization[47]. In catechol-based systems, redox cycling drives the switch between catechol and quinone species, processes that are often accompanied by measurable optical changes. Capturing these changes in real time is essential for coupling electrochemical input to molecular-level information.

In this chapter, two subsections of temporally resolved redox behavior are investigated. The first subsection focuses on examining redox cycling behavior of both catechol-functionalized hydrogels through absorbance-based measurements obtained using both the Pine instrument as a ground truth device against the tested RGB-based image analysis framework. This comparison establishes whether simplified image-derived RGB optical signals can reproduce trends observed in wavelength-resolved spectroscopy during dynamic electrochemical operation.

The section subsection focuses on Cat-PEG and its previously reported dual optical switching capability in both absorbance and fluorescence modalities[35]. Due to the limited nature of the Pine instrument to capture additional optical modalities, the image-based framework is leveraged to monitor both absorbance and fluorescence simultaneously during redox cycling. Unlike absorbance, which reflects bulk optical attenuation, fluorescence provides complementary information related to excited-state processes and molecular environment. This multimodal

imaging approach therefore offers a more comprehensive understanding of catechol redox behavior than can be achieved with conventional spectroelectrochemical techniques alone.

4A: Redox Switching Absorbance Analysis

Absorbance Behavior in Redox Switching

Previous works have highlighted a fundamental aspect of electrochemical redox processes: electrons are not directly soluble and cannot be transferred from the electrode to catechol molecules without an intermediary[48]. To overcome this limitation, diffusible redox mediators are often employed to shuttle electrons between the electrode and the grafted film[49]. This mediated redox cycling is schematically illustrated in **Fig. 4.1**.

Under reducing potential applied at the electrode surface, $Ru(NH_3)_6Cl_3$ (Ru 3^+) can undergo redox cycling: it is reduced at the electrode, diffuses into the hydrogel film, and subsequently oxidized by donating electrons to the grafted catechol molecules[7]. The oxidized Ru 3^+ then diffuses back to the electrode, where it can be reduced again, thereby progressively switching the grafted molecules to their reduced (catecholic) state. Similarly, under oxidative potentials, ferrocene dimethanol (Fc) can undergo analogous redox cycling, transferring electrons to switch the grafted molecules to their oxidized (quinone) state. Both mediators can coexist in the same solution because each is electrochemically activated only when the applied potential approaches its respective formal potential (E^0), a characteristic thermodynamic property of each mediator[50].

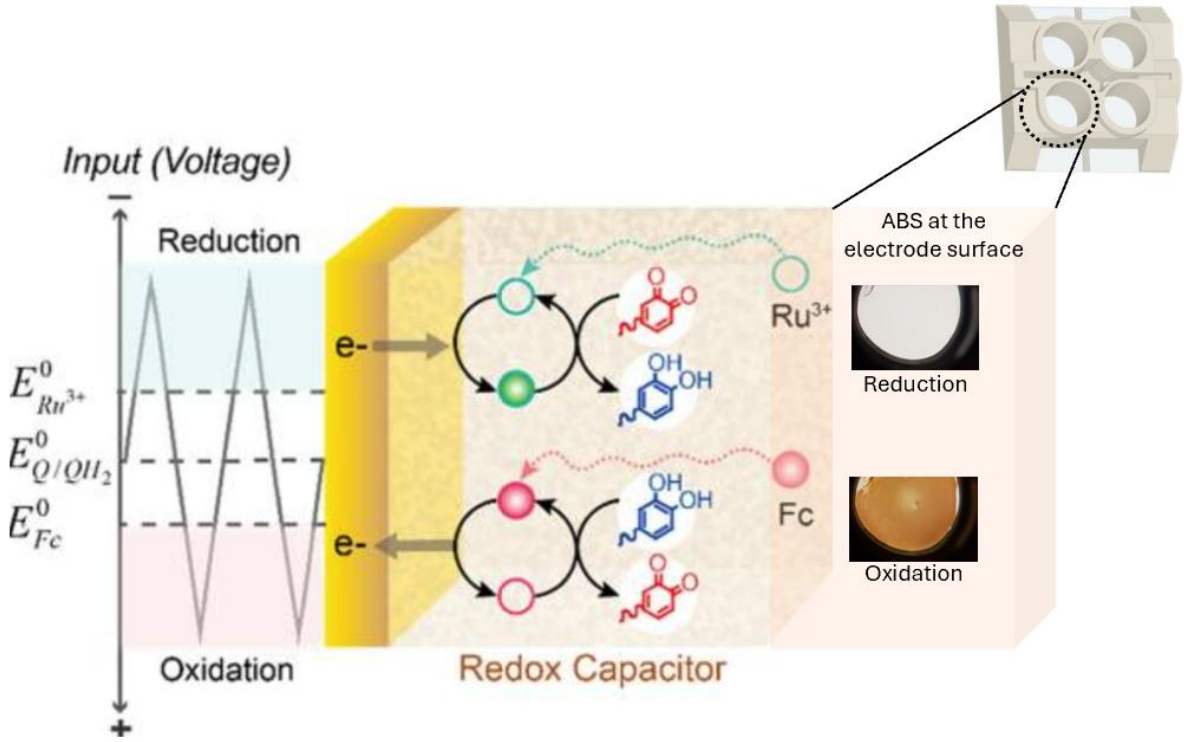

Figure 4.1: Redox-Based Absorbance Switching

During redox cycling, changes in oxidation state of the grafted catechol molecules are accompanied by measurable alterations in optical absorbance. As the electrode potential drives reduction via the Ru^{3+} mediator, catechol groups are converted to their reduced form, leading to characteristic decreases in absorbance at wavelengths associated with the oxidized quinone species. Conversely, when oxidative potentials are applied and Fc facilitates electron transfer, catechol groups are converted back to the oxidized quinone state, producing a corresponding increase in absorbance. These absorbance changes provide a direct, optical readout of the redox state of the hydrogel and can be tracked continuously over time.

By monitoring absorbance this way, the dynamic switching of the grafted molecules can be quantified, revealing both the flow of electron transfer and the efficiency of the mediator-driven redox processes. Because absorbance measurements integrate over the entire electrode area, they

provide a spatially averaged view of the molecular switching, which can be directly compared between the spectroelectrochemical reference instrument and the camera-based RGB analysis framework. This comparison allows evaluation of whether simplified image-based measurements capture the same temporal trends in full-spectrum data.

Phase Plane Analysis

To monitor the absorbance response of catechol-functionalized hydrogels during redox cycling, CV was conducted in both the Pine instrument and the camera-based setup, using the parameters described in the Experimental Methods section. **Fig. 4.2a** shows the applied potential plots scanning between oxidative and reductive potential along with the corresponding detrended charge-time and absorbance-time data (see **Appendix** for raw data). In both systems, absorbance changes were observed to be in phase with the applied electrochemical input: as the quinone groups were oxidized, an increase in absorbance was detected across all catechol-functionalized gels. In the Pine instrument, wavelength-resolved data aligned with the representative RGB channels measured in the camera-based setup, demonstrating consistent optical trends between the two modalities.

Phase plane plots were further used to examine the relationship between electrical and optical signals during operando measurements (**Fig. 4.2b**). In these plots, both charge and absorbance (wavelength or filter specific) are plotted against the applied potential, revealing a clear qualitative agreement in the shapes of the responses. This correspondence was observed for both catechol-functionalized materials and across instruments, confirming that the simplified RGB-based image analysis framework captures the same charge-dependent optical trends as full-spectrum spectroscopic measurements.

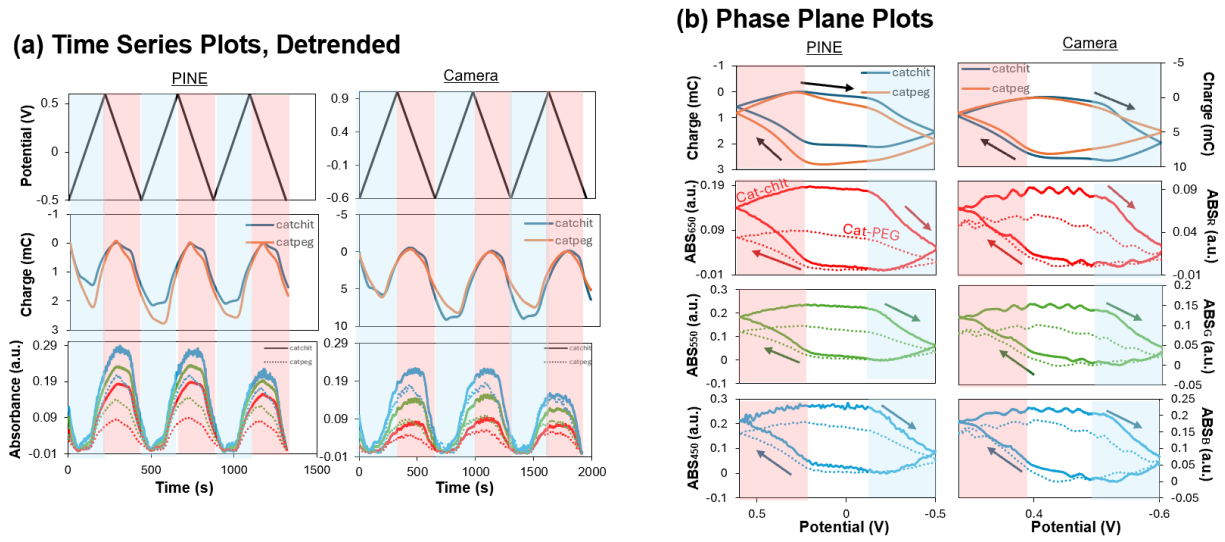

Figure 4.2: Phase Plane Analysis. (a) Time-series plots and (b) phase plane plots of both cat-chit and cat-PEG in either experimental setup, all data has been detrended.

Cross-Modal Correlation

To quantify the trends observed qualitatively in **Fig. 4.2**, a cross-modal analysis similarly to that employed in Chapter 3 was performed. Instead of focusing on slopes, a cross-modal amplitude ratio ($Amp._{CM}$) was calculated using the following relationship:

$$Amp._{CM} = \frac{Amp._{optical}}{Amp._{electrical}}$$

Here, $Amp._{electrical}$ represents the amplitude measured from the electrical phase-plane plot of a given functionalized hydrogel, while $Amp._{optical}$ corresponds to the amplitude extracted from the optical phase-plane plot for the same material at each respective wavelength or RGB color channel (**Fig. 4.3a)**. This approach generates a distinct $Amp._{CM}$ for every wavelength or color channel across each functionalized hydrogel.

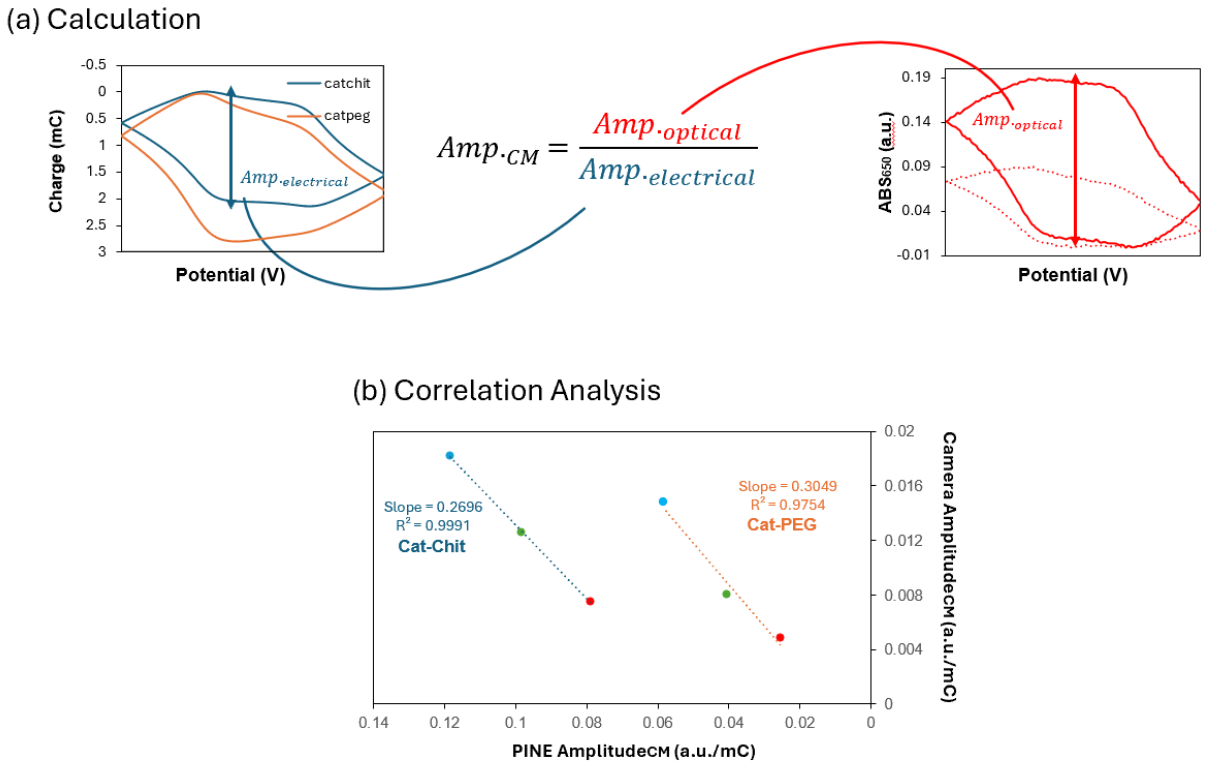

Figure 4.3: Correlation Analysis.

A subsequent correlation analysis was then performed to evaluate the agreement between the reference Pine instrument and the camera-based image analysis framework, allowing assessment of how well the simplified RGB-based approach captures the quantitative amplitude of redox-driven optical change (**Fig. 4.3b**). Consistent with the results reported in Chapter 3, both functionalized hydrogels exhibited strong correlations, with R^2 values exceeding 0.97. This indicates that over 97% of the variance in the RGB-derived data is explained by the corresponding spectral measurements, further confirming the high degree of quantitative agreement between the two measurement modalities.

4B: Redox Switching Multimodal Analysis

Multimodal Optical Behavior in Redox Switching

A key advantage of the camera-based image analysis framework is its ability to support multimodal optical imaging. In addition to tracking absorbance, the imaging platform enables simultaneous monitoring of fluorescence throughout electrochemically induced redox cycling, providing access to complementary optical information.

The underlying electrochemical behavior follows the mediator-driven redox cycling mechanism described previously, in which soluble species facilitate electron transfer between the electrode and the grafted film. While absorbance increases during oxidation as catechol groups are converted to quinone, fluorescence exhibits an inverse response, increasing during reduction as quinone is converted back to catechol. This out-of-phase relationship between absorbance and fluorescence highlights the presence of distinct optical signatures associated with different redox states and demonstrates the added analytical value of multimodal imaging.

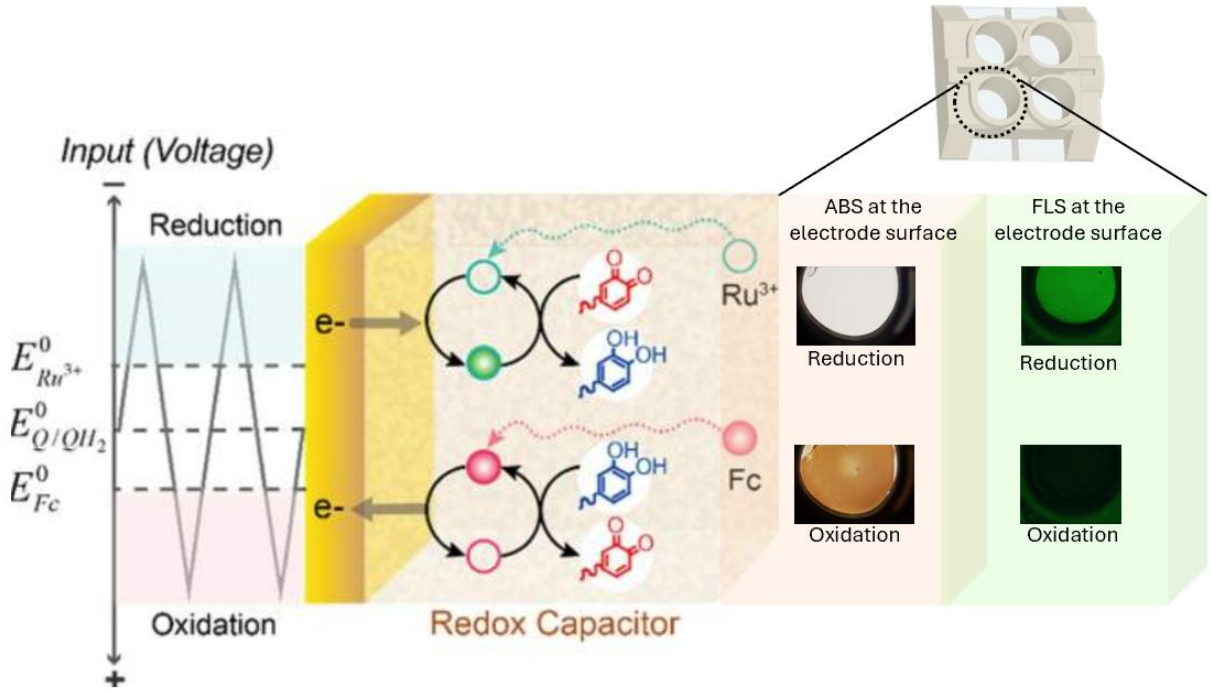

Figure 4.4: Redox-Based Multimodal Optical Switching

Image-Based Multimodal Monitoring

To monitor fluorescent behavior in Cat-chit and Cat-PEG during redox cycling, the same CV protocol described in Chapter 4a was conducted using only the camera-based imaging platform. **Fig. 4.5a** shows the applied potential waveform alongside the corresponding detrended current-time, charge-time, and fluorescence-time data. In this system, fluorescence was out of phase relative to the applied electrochemical input. Specifically, as the catechol groups were reduced, an increase in fluorescence intensity was observed in Cat-PEG. In contrast, cat-Chit displayed no measurable fluorescence modulation during redox cycling, highlighting the selective sensitivity of the imaging approach and its ability to differentiate material-specific optical behavior.

To further emphasize the spatial and visual nature of this technique, **Fig. 4.5b** presents representative microscope images captured at peak oxidation and reduction potentials. These

images directly illustrate the redox-dependent fluorescence switching observed in cat-PEG, as well as the absence of fluorescence response in Cat-chit. The phase relationship is evident both qualitatively in the images and quantitatively in the extracted intensity profiles, where fluorescence intensity is inversely correlated with charge.

To directly compare multimodal optical responses, absorbance and fluorescence signals for cat-PEG were plotted together (**Fig. 4.5c**). Absorbance increases in phase with catechol oxidation, while fluorescence intensity increases during reduction of quinone species. This results in a clear 180° phase offset between absorbance and fluorescence signals, demonstrating that each modality probes distinct aspects of the redox state. Together, these results highlight the capability of the camera-based platform to capture complementary, redox-dependent optical signatures via absorbance and fluorescence measurements.

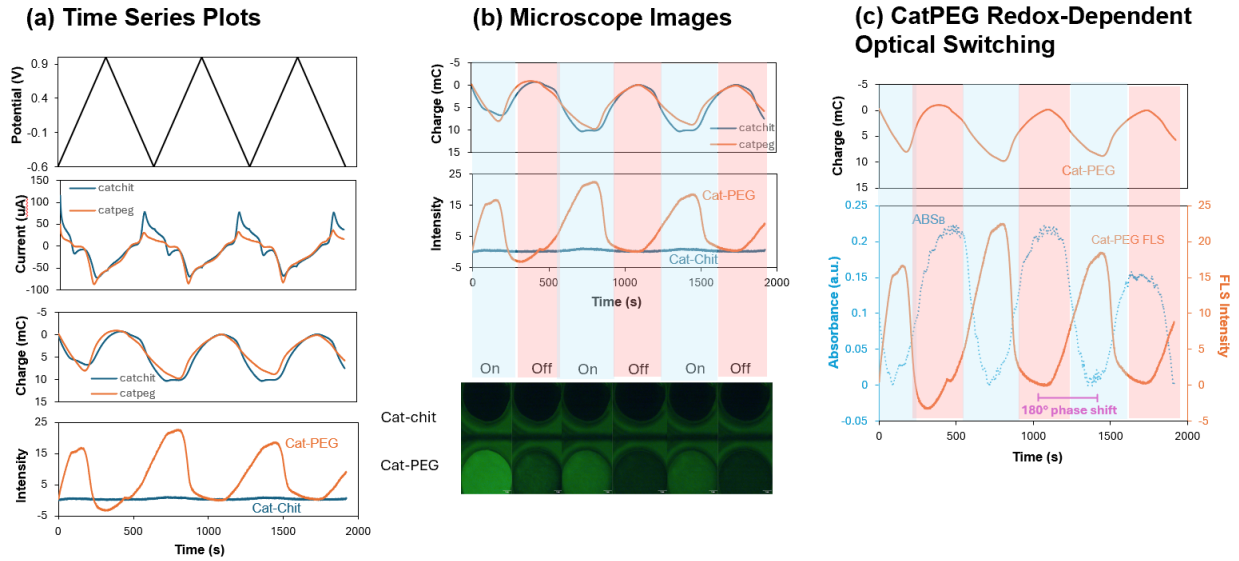

Figure 4.5: Multimodal Optical Monitoring. (a) Time series plots and corresponding (b) microscope images of cat-chit and cat-PEG, data has been detrended. (c) Overlay of both absorbance and fluorescence switching in cat-PEG, data has been detrended.

Chapter 5: Spatial Resolution in Patterned Electrode Geometries

Motivation

In this chapter, patterned electrodes were employed to highlight the enhanced capability to detect spatially resolved gradients afforded by the camera-based image analysis framework. Unlike spectrometers, which provide spatially averages signals, the imaging approach enables localized optical responses to be resolved across complex electrode geometries.

To demonstrate this capability, dual working electrodes were fabricated on a single ITO substrate using the laser engraving procedures described in the experimental methods. In this configuration, independent electrochemical potentials can be applied simultaneously to each electrode, enabling opposing redox states to be generated within the same field of view. This represents a distinct advancement over previous experiments, where all regions of the well were subjected to a uniform potential.

By adapting the ImageJ analysis macro to define separate regions of interests (ROIs) for each electrode, spatially resolved optical signals can be extracted independently. This enables direct visualization of redox behavior, where opposing fluorescence responses can be observed as a function of the cat-PEG redox state under different applied potentials.

Patterned Electrode Geometry

The electrode used in this study was specifically designed to enable spatially resolved electrochemical control within a single well. The patterned ITO substrate consisted of two

interdigitated, comb-like working electrodes that converge at the center of the device (**Fig. 5.1**). This geometry maximizes the proximity of independently controlled regions while maintaining electrochemical isolation between electrodes.

The same ITO glass substrate used in the 4-well platform described in Chapters 3 and 4 was adapted for this configuration, with the surface divided into two working electrodes rather than four. **Fig. 5.1a** shows a top-down view of the spectroelectrochemical platform, corresponding to the perspective captured by the imaging system, with both working electrodes highlighted. **Fig. 5.1b** presents an angled view of the device, identifying the placement of the working, counter, and reference electrodes. This overall set-up retains the same counter and reference electrode configuration, as well as the same platform architecture as the previously described 4-well system.

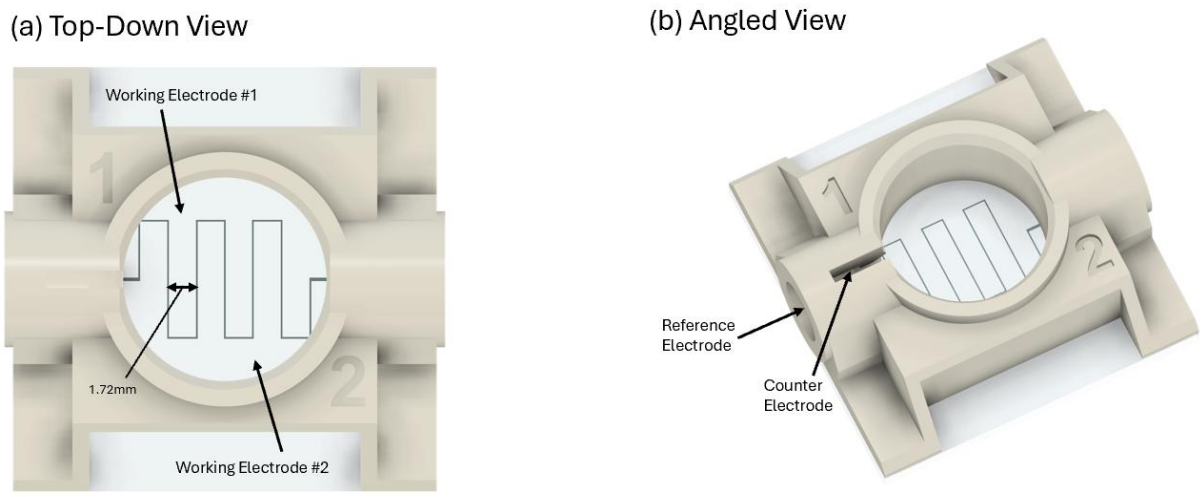

Figure 5.1: Patterned Electrode Views

Operando Electrode Modulation

Fabrication of Film

Fabrication of Cat-PEG on the patterned electrode follows the procedures outlined in the **Experimental Methods** section, with minor adaptations for the dual-electrode configuration. The protocol for sealing the 3D-printed housing to the two-electrode ITO coated glass remained unchanged.

For electrodeposition, 500uL of the deposition solution (50mM Catechol, 50 mg mL^{-1} 4-arm thiol PEG) was micropipetted into the single-well. The reference, counter, and both working electrode leads were connected from the spectroelectrochemical platform to the electrochemical analyzer. An anodic potential of +1.0V was then applied for 5 minutes to both working electrodes simultaneously, resulting in formation of a uniform cat-PEG hydrogel layer across each electrode surface (**Fig. 5.2 left**). Following this, the deposition solution was removed and replaced with PB for a 30-minute incubation period. During incubation, the film becomes reduced because of the neutral pH of PB, seen under fluorescence imaging(**Fig. 5.2 right**).

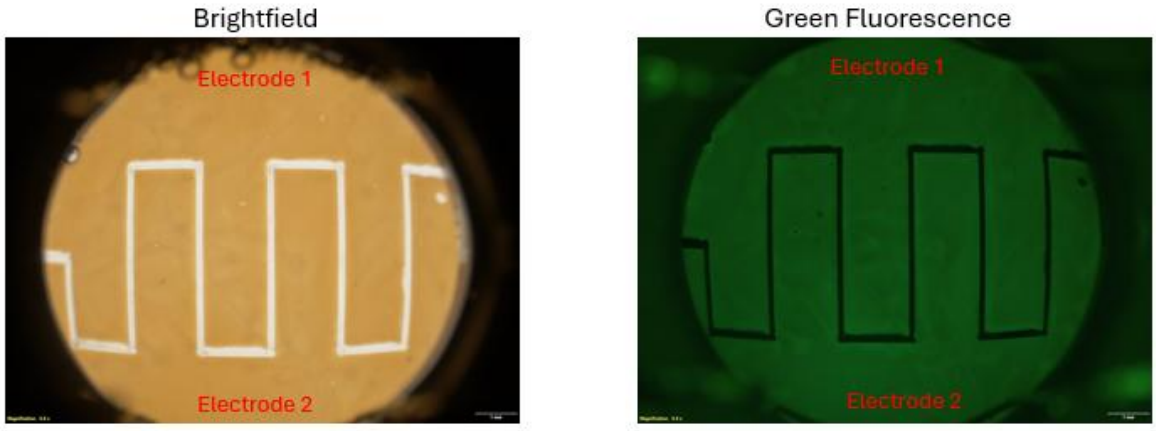

Figure 5.2: After-Deposition Images

Redox Probing

To demonstrate redox-switching behavior within the patterned electrode system, a solution containing both mediators (0.5mM Ru^{3+}, 0.5mM Fc) was added to the single-well device. Chronocoulometry (CC) was then performed by applying alternating oxidative (+1.0V) and reductive (-0.6V) potentials in three pulse intervals of 2 minutes (120 s) each (**Fig 5.3 top and bottom**). Importantly, the two working electrodes received out-of-phase pulse sequences, such that one electrode experienced an oxidative potential while the other a reductive potential.

The resulting charge-time and fluorescence-time responses are shown in **Fig. 5.3**, highlighting the redox-dependent fluorescent behavior of cat-PEG. Consistent with earlier observations, fluorescence intensity acts inversely with catechol oxidation state, increasing under reductive conditions and decreasing under oxidative conditions. Because the electrodes received opposing potential, this results in spatially distinct fluorescence responses across the two electrode surfaces.

This behavior is further illustrated through representative microscope images captured at the beginning of each experiment and at the end of each potential pulse (**Fig. 5.3** middle). Initially, both electrodes exhibit minimal fluorescence, indicating similar redox states. Following the first pulse interval, a clear divergence is observed: the electrode subjected to the reductive potential displays a pronounced increase in fluorescence intensity, while the electrode under oxidative potential remains comparatively unchanged. This alternating pattern persists throughout subsequent pulse intervals, with fluorescence switching between electrodes in accordance with the opposing applied potential.

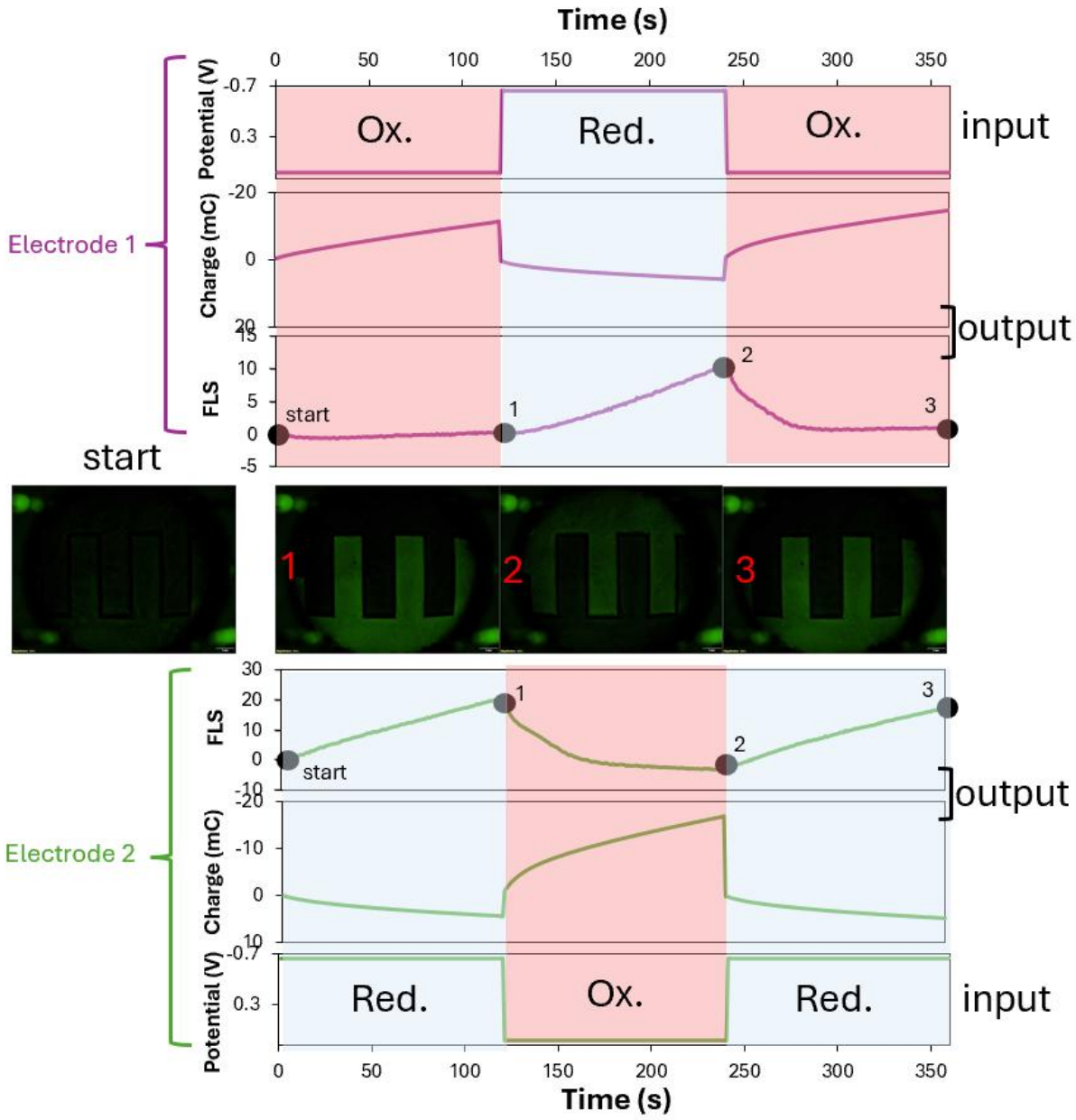

Figure 5.3: Redox-Dependent Electrode Modulation. Chronocoulometry experiments to create potential pulses for a period of 120 seconds each, alternating between oxidative and reductive potentials.

Overall, the results presented in this chapter highlight the unique capability of the camera-based image analysis framework to resolve spatially complex electrochemical behavior that is inaccessible via conventional spectroscopy. By integrating independently addressable electrodes

within a single viewpoint, this approach enables direct visualization of spatiotemporally varying redox states, revealing distinct optical responses under opposing electrochemical conditions. The ability to capture these spatially heterogenous signals in real time, while maintaining both absorbance and fluorescence modalities, provides a significant advantage over traditional methods that rely on spatially averaged measurements. This chapter demonstrates that image-based analysis not only preserves key electrochemical and optical trends (as seen in Chapters 3 and 4), but also extends capability into the spatial domain, offering a powerful platform for studying complex, spatially heterogenous spectroelectrochemical systems.

Chapter 6: Conclusion

Key Findings

Chapter 3 of this thesis investigated the electrochemical fabrication of two catechol-functionalized hydrogels (Cat-chit and Cat-PEG) across two experimental setups. The primary objective was to evaluate whether the newly developed camera-based image analysis framework could produce filter-dependent optical information analogous to wavelength-dependent data obtained from a spectroelectrochemical reference instrument. The results demonstrated strong agreement between the two approaches, with both conjugation chemistries exhibiting consistent charge-dependent optical behavior across measurement instruments.

Chapter 4 built upon these key findings by probing the redox-dependent optical switching of the fabricated hydrogels. The first section compared absorbance changes during redox cycling in both the reference instrument and the image-based framework, further confirming close agreement between the two methods. The second section leveraged the multimodal capability of the imaging approach to simultaneously monitor absorbance and fluorescence. While cat-chit exhibited no fluorescence response, cat-PEG displayed both absorbance and fluorescence signals, with a clear 180° phase offset between the two.

Chapter 5 introduced spatial complexity using a patterned electrode system consisting of two independently controlled working electrodes within a single well. Using cat-PEG functionalized electrodes, opposing electrochemical potentials were applied simultaneously to generate spatially distinct redox environments. The camera-based method successfully resolved these localized responses, with fluorescence intensity increasing under reductive conditions and decreasing under oxidative conditions.

Advantages and Limitations of the Framework

This work highlights the tradeoff between traditional spectroscopic instrumentation and the proposed image-based analysis approach, emphasizing a balance between spectral resolution and spatial and temporal capability. Conventional spectroscopy provides highly resolved, wavelength-dependent information across the full optical spectrum, enabling a detailed characterization of molecular features[51]. In contrast, the image-based framework reduces this complexity by compressing spectral information into RGB channels, resulting in a loss of fine spectral detail at specific wavelengths.

Despite this limitation, the image-based approach offers significant advantages in both temporal and spatial resolution. In contrast to conventional spectroscopy that requires sequential wavelength scanning, limiting acquisition speed, this approach leverages discrete filters to capture sufficient spectral information without sacrificing temporal resolution. This enables continuous, high-frequency image acquisition on sub-second timescales with flexible synchronization to electrical outputs. Importantly, we demonstrate the feasibility of the three filters to resolve relevant spectral differences, as shown by distinguishing between the formation of two chemically distinct catechol-conjugated films. In addition, the spatial capability of imaging allows for region-specific analysis, enabling a unique visualization of heterogenous environments across complex electrode geometries. This capability is not accessible within conventional spectroscopy, which relies on spatially averaged measurements.

Together, these results illustrate that while the RGB-based image analysis framework does not replace full-spectrum spectroscopy, it provides a complementary approach that prioritizes speed, simplicity, and cost. Therefore, the choice between methods depends solely on the specific

analytical needs of a system, with the imaging platform offering distinct advantages when studying dynamic and spatially complex processes.

Future Work

Gel-Dependent Modulation

While the patterned electrode work focused on redox switching within a single catechol-functionalized hydrogel (Cat-PEG), future studies could explore systems containing multiple materials within the same device. For example, depositing distinct catechol-functionalized hydrogels (cat-chit or cat-PEG) on separate electrodes within a single well would enable direct, simultaneous comparison of their redox-dependent optical responses. Coupled with independently controlled or synchronized electrical inputs, this approach would allow for electrode-specific modulation of different conjugation chemistries in a shared environment. Such experiments could provide deeper insight into how variations in grafting chemistry influence redox behavior under shared experimental conditions.

Biomimetic Memory Material

An additional direction could be investigating the persistence of redox states in catechol-functionalized hydrogels, with the goal of developing biomimetic memory-like materials. By applying pulsed electrochemical inputs and subsequently removing the applied potential, the temporal stability of induced optical states (fluorescence or absorbance) can be monitored. Using the imaging platform, the retention or decay of these signals could be tracked in both time and space, providing insight into the extent to which these materials contain “redox memory.”

Biological Sensing

Building on the observed redox-dependent optical switching of Cat-PEG, future work could explore its application as a sensing platform. The material may be used to detect the presence of redox-active species, such as antioxidants or pro-oxidants, which can interact with grafted catechol groups and induce measurable optical changes. Additionally, incorporation of biological systems, such as living cells, could enable monitoring of cell-mediated redox activity at material interfaces. In such cases, cellular processes that alter local redox environment may lead to detectable decreases in absorbance or increases in fluorescence, providing a foundation for developing image-based, electrochemically responsive biosensing platforms.

Appendices

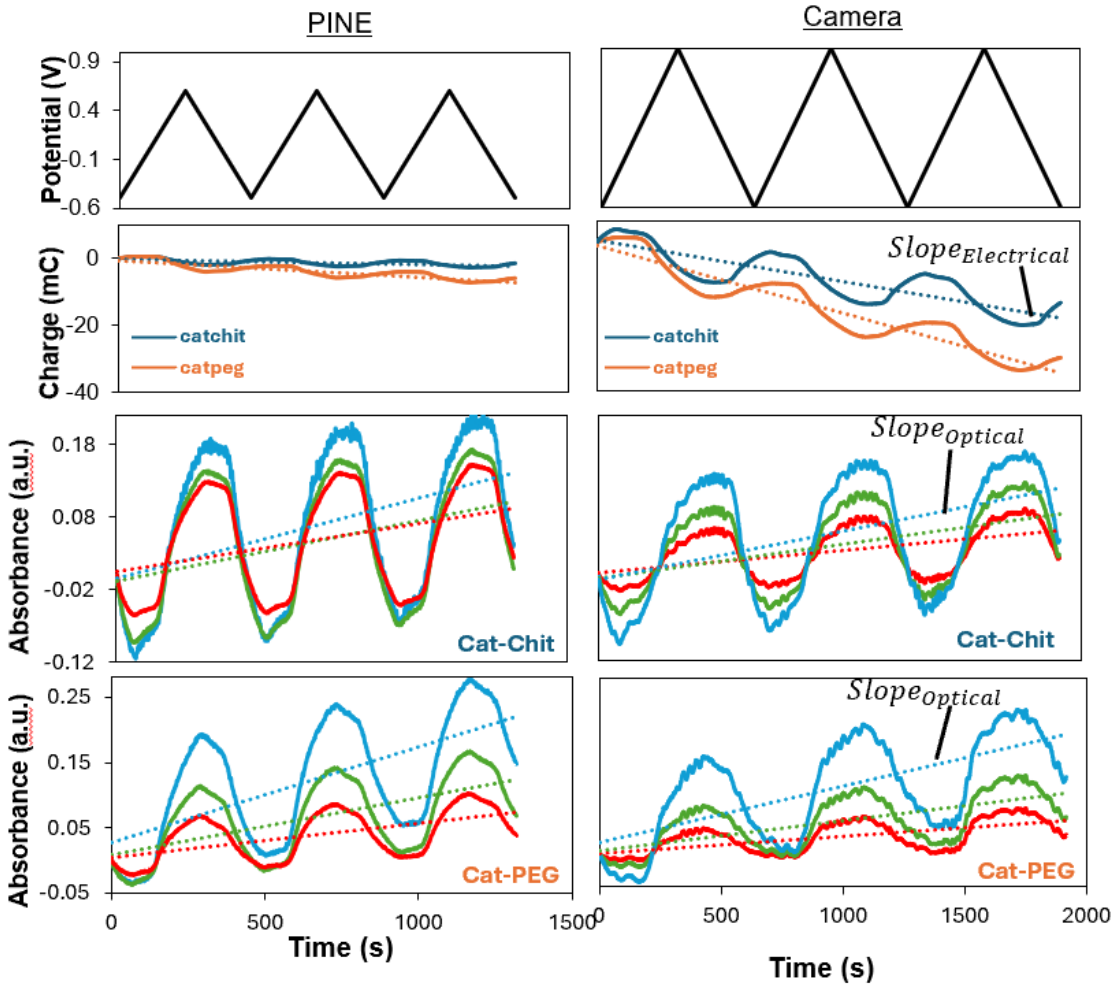

Raw data from Chapter 4: Phase Plane Analysis before detrending was applied. Detrending was conducted using OriginPro's Peaks and Baseline toolbox, using adjacent-averaging smoothing with 4 user-defined points of the corresponding minima.

Bibliography

1. Stenzel, M. H. Bioconjugation Using Thiols: Old Chemistry Rediscovered to Connect Polymers with Nature's Building Blocks. *ACS Macro Lett.* **2**, 14–18 (2013).
2. Mitchell, J. S., Wu, Y., Cook, C. J. & Main, L. Direct ring conjugation of catecholamines and their immunological interactions. *Bioconjug Chem* **18**, 268–274 (2007).
3. Bolaños-Cardet, J. *et al.* The Redox Properties of Polyphenols and Their Role in ROS Generation for Biomedical Applications. *Angewandte Chemie International Edition* **65**, e13698 (2026).
4. Kutyrev, A. A. & Moskva, V. V. Nucleophilic reactions of quinones. *Russ. Chem. Rev.* **60**, 72 (1991).
5. Chen, C., Li, D., Yano, H. & Abe, K. Bioinspired hydrogels: Quinone crosslinking reaction for chitin nanofibers with enhanced mechanical strength via surface deacetylation. *Carbohydrate Polymers* **207**, 411–417 (2019).
6. Saiz-Poseu, J., Mancebo-Aracil, J., Nador, F., Busqué, F. & Ruiz-Molina, D. The Chemistry behind Catechol-Based Adhesion. *Angewandte Chemie International Edition* **58**, 696–714 (2019).
7. Wu, S. *et al.* Catechol-Based Capacitor for Redox-Linked Bioelectronics. *ACS Appl. Electron. Mater.* **1**, 1337–1347 (2019).
8. Sedó, J., Saiz-Poseu, J., Busqué, F. & Ruiz-Molina, D. Catechol-Based Biomimetic Functional Materials. *Advanced Materials* **25**, 653–701 (2013).
9. Uchimiya, M. & Stone, A. T. Reversible redox chemistry of quinones: Impact on biogeochemical cycles. *Chemosphere* **77**, 451–458 (2009).

10. Kim, E. *et al.* Biomimetic Redox Capacitor To Control the Flow of Electrons. *ACS Appl. Mater. Interfaces* **16**, 61495–61502 (2024).

11. Melanin Pigmentation in Mammalian Skin and Its Hormonal Regulation | Physiological Reviews | American Physiological Society. https://journals.physiology.org/doi/full/10.1152/physrev.00044.2003?utm_campaign=DSL_tru-alchemy-glow-serum-review.

12. Kollias, N., Sayre, R. M., Zeise, L. & Chedekel, M. R. New trends in photobiology: Photoprotection by melanin. *Journal of Photochemistry and Photobiology B: Biology* **9**, 135–160 (1991).

13. Kim, E. *et al.* Enlisting electrochemistry to reveal melanin's redox-related properties. *Materials Advances* **5**, 3082–3093 (2024).

14. Studies on Synthetic and Natural Melanin and Its Affinity for Fe(III) Ion - Costa - 2012 - Bioinorganic Chemistry and Applications - Wiley Online Library. https://onlinelibrary.wiley.com/doi/full/10.1155/2012/712840.

15. Melanin - Unravelling the Structure and Function Through Synthesis | Journal of the American Chemical Society. https://pubs.acs.org/doi/full/10.1021/jacs.0c12322.

16. Diversity of human hair pigmentation as studied by chemical analysis of eumelanin and pheomelanin - Ito - 2011 - Journal of the European Academy of Dermatology and Venereology - Wiley Online Library. https://onlinelibrary.wiley.com/doi/full/10.1111/j.1468-3083.2011.04278.x.

17. Ozeki, H., Ito, S., Wakamatsu, K. & Thody, A. J. Spectrophotometric Characterization of Eumelanin and Pheomelanin in Hair. *Pigment Cell Research* **9**, 265–270 (1996).

18. Del Bino, S. *et al.* Chemical analysis of constitutive pigmentation of human epidermis reveals constant eumelanin to pheomelanin ratio. *Pigment Cell & Melanoma Research* **28**, 707–717 (2015).

19. Hearing, V. J. Determination of Melanin Synthetic Pathways. *Journal of Investigative Dermatology* **131**, E8–E11 (2011).

20. Cao, W. *et al.* Biomimetic pheomelanin to unravel the electronic, molecular and supramolecular structure of the natural product. *Chemical Science* **14**, 4183–4192 (2023).

21. Kaxiras, E., Tsolakidis, A., Zonios, G. & Meng, S. Structural Model of Eumelanin. *Phys. Rev. Lett.* **97**, 218102 (2006).

22. Liu, S. *et al.* Melanin-Inspired Composite Materials: From Nanoarchitectonics to Applications. *ACS Appl. Mater. Interfaces* **16**, 3001–3018 (2024).

23. Solano, F. Melanin and Melanin-Related Polymers as Materials with Biomedical and Biotechnological Applications—Cuttlefish Ink and Mussel Foot Proteins as Inspired Biomolecules. *International Journal of Molecular Sciences* **18**, (2017).

24. The Chemistry of Bioinspired Catechol(amine)-Based Coatings | ACS Biomaterials Science & Engineering. https://pubs.acs.org/doi/full/10.1021/acsbiomaterials.9b00281.

25. Zhang, K. *et al.* Efficient catechol functionalization of biopolymeric hydrogels for effective multiscale bioadhesion. *Materials Science and Engineering: C* **103**, 109835 (2019).

26. Lhenry, S., Leroux, Y. R. & Hapiot, P. Use of Catechol As Selective Redox Mediator in Scanning Electrochemical Microscopy Investigations. *Anal. Chem.* **84**, 7518–7524 (2012).

27. Ryu, J. H., Hong, S. & Lee, H. Bio-inspired adhesive catechol-conjugated chitosan for biomedical applications: A mini review. *Acta Biomaterialia* **27**, 101–115 (2015).

28. Li, J. *et al.* Interactive Materials for Bidirectional Redox-Based Communication. *Advanced Materials* **33**, 2007758 (2021).

29. Chen, C.-Y. *et al.* 3D Printed Spectroelectrochemical Platform for Redox-Based Bioelectronics. *Small Methods* **9**, e2401843 (2025).

30. Zhai, Y., Zhu, Z., Zhou, S., Zhu, C. & Dong, S. Recent advances in spectroelectrochemistry. *Nanoscale* **10**, 3089–3111 (2018).

31. Kaim, W. & Fiedler, J. Spectroelectrochemistry: the best of two worlds. *Chemical Society Reviews* **38**, 3373–3382 (2009).

32. Atifi, A. Introducing a Machine Learning Approach to Uncover Fundamental Electrochemical Insights from in-Situ Spectroelectrochemical Data. *Meet. Abstr.* **MA2025-02**, 2615 (2025).

33. Tan, J., Lien, J.-M. & Gingold, Y. Decomposing Images into Layers via RGB-Space Geometry. *ACM Trans. Graph.* **36**, 7:1-7:14 (2016).

34. Yang, J., Stuart, M. A. C. & Kamperman, M. Jack of all trades: versatile catechol crosslinking mechanisms. *Chemical Society Reviews* **43**, 8271–8298 (2014).

35. Chen, C.-Y. *et al.* 3D Printed Spectroelectrochemical Platform for Redox-Based Bioelectronics. *Small Methods* **9**, e2401843 (2025).

36. Jia, Y. *et al.* From RGB to Spectrum for Natural Scenes via Manifold-Based Mapping. in *2017 IEEE International Conference on Computer Vision (ICCV)* 4715–4723 (2017). doi:10.1109/ICCV.2017.504.

37. Santos, E. & Schmickler, W. On the timescale of electrochemical processes. *Electrochimica Acta* **498**, 144659 (2024).

38. Wu, S. *et al.* Catechol-Based Molecular Memory Film for Redox Linked Bioelectronics. *Advanced Electronic Materials* **6**, 2000452 (2020).

39. Serrà, A. & García-Torres, J. Electrochemistry: A basic and powerful tool for micro- and nanomotor fabrication and characterization. *Applied Materials Today* **22**, 100939 (2021).

40. Winkler, S., Saracevic, E., Bertrand-Krajewski, J.-L. & Torres, A. Benefits, limitations and uncertainty of in situ spectrometry. *Water Sci Technol* **57**, 1651–1658 (2008).

41. Prince, A. B. Absorption Spectrophotometry. in *Methods of Soil Analysis* 866–878 (John Wiley & Sons, Ltd, 1965). doi:10.2134/agronmonogr9.2.c4.

42. Kosri, E., Ibrahim, F., Thiha, A. & Madou, M. Micro and Nano Interdigitated Electrode Array (IDEA)-Based MEMS/NEMS as Electrochemical Transducers: A Review. *Nanomaterials* **12**, (2022).

43. Cole, K. D. *et al.* NIST Spectroscopic Measurement Standards. *Biopharm Int* **31**, 22–34 (2018).

44. Branch, S. D. *et al.* Optically Transparent Thin-Film Electrode Chip for Spectroelectrochemical Sensing. *Anal. Chem.* **89**, 7324–7332 (2017).

45. Gutzen, R. Lifting the Purple Haze. *Robin Gutzen* http://robingutzen.com/2020-11-05-color_spaces/ (2020).

46. Microscopy Light Filters: Types, Construction & Selection Guide | Evident. https://evidentscientific.com/en/microscope-resource/knowledge-hub/lightandcolor/filtersintro.

47. Yammine, P. *et al.* Recent Advances in Applied Electrochemistry: A Review. *Chemistry* **6**, 407–434 (2024).

48. Kim, E. *et al.* Electrochemistry as a Tool for Redox-Based Bio-Information Processing. *Advanced Science* **12**, e10184 (2025).

49. Shao, W. *et al.* The Use of Redox Mediators in Electrocatalysis and Electrosynthesis. *Chemistry – An Asian Journal* **18**, e202201093 (2023).

50. Prince, R. C., Linkletter, S. J. & Dutton, P. L. The thermodynamic properties of some commonly used oxidation-reduction mediators, inhibitors and dyes, as determined by polarography. *Biochim Biophys Acta* **635**, 132–148 (1981).

51. Scientific, T. F. Monitoring Reactions Through UV-Visible Spectroscopy | Spectroscopy Online. https://www.spectroscopyonline.com/view/monitoring-reactions-through-uv-visible-spectroscopy (2026).